

Dynamics of a periodic XY chain coupled to a photon mode

S. Varbev, I. Boradjiev,* H. Tonchev, and H. Chamati

Institute of Solid State Physics, Bulgarian Academy of Sciences, Tzarigradsko chaussée 72, 1784 Sofia, Bulgaria

(Dated: September 18, 2019)

We study the real-time dynamics of a periodic XY system exposed to a composite field comprised of a constant homogeneous magnetic and a quantized circularly polarized electromagnetic fields. The interaction between the quantized mode and spin-magnetic moments is modeled by the Dicke Hamiltonian. The rotating wave approximation is applied and the conditions for its validity are discussed. It is shown that if at the beginning of the dynamic process all of the excitations are contained in the field then, in the regime of large detuning, the main evolutionary effect is the oscillations of the excitations between the zero-momentum modes of the chain and the field. Accordingly, the reduced photon number and magnetization per site reveal a sort of oscillatory behavior. Effective Hamiltonians approximating the short-time dynamics of the actual problem for small number of excitations and large detuning are introduced. The resonance case is considered in the context of photon emission from the chain initially prepared in the (partially) excited state. In particular, it is demonstrated in the framework of a specific example that the superradiant behavior can be presented in the beginning of the emission, when the evaluation starts from maximally excited XY chain. The model is potentially applicable to problems such as spin chain/linear molecular aggregates in a single-mode cavity.

PACS numbers: S 75.10.Jm, 75.10.Pq, 37.30.+i

I. INTRODUCTION

Light-matter interaction is an important mean in condensed matter physics. It provides useful insights into the material's behavior and can be used to manipulate its physical properties for engineering new devices for different applications. In particular, the manipulation of magnetic ordering and thus the magnetic properties of spin systems by laser pulses has attracted an increasing interest due to potential applications in spintronics and quantum information, see e.g. [1–3] and references therein. For practical purposes, a commonly used approach consists in using focused ultra-short laser pulses [4, 5] to control, more generally, the dynamics in magnetic systems, such as, ferromagnetic [6], antiferromagnetic [7] or ferrimagnetic materials [8]. Thus, a single ultrafast laser pulse can permanently affect the dynamics of a spin even in the absence of a magnetic field [9, 10]. This would not have been possible without the technological advancement that made the synthesis of low dimensional spin systems achievable [11], on one hand and a better understanding of light-matter interaction to bring new tools for manipulating quantum states – a key ingredient for the ultimate goal of quantum information – the quantum computer, on the other. Furthermore, the light-matter interaction can be used to model quantum simulators (see e.g. [2] and references therein), to engineer a new generation of atomic clocks [12], etc.

In quantum optics, the basic models describing a system consisting of two-level atom(s) interacting with a single mode of quantized electromagnetic field are: The Jaynes-Cummings [13], the Tavis-Cummings [14], and the Dicke [15] models. The Dicke model describes a set of independent two-level systems interacting with a photon mode.

Within the Rotating Wave Approximation (RWA) the Dicke model reduces to the Tavis-Cummings model, which in the case of a single atom turns out to be the Jaynes-Cummings model. Over the years, these models have been and are continuously studied and extended in a great many directions, such as transient and steady-state superradiance [15, 16], superabsorption [17], the validity of RWA [18, 19], the high detuning limit [20, 21], the inhomogeneous versions of the models [22], etc. When switching on the interaction among the constituting atomic spins in the Dicke (Tavis-Cummings) model it is possible to end up with a physically rich system, where light and matter interact [23–26]. Depending on the specificity of the problem different ways can be used to (effectively) model the interaction. A widely used spin model is the exactly soluble quantum XY model with nearest-neighbor interaction [27–29].

In this paper we study the behavior of the quantum XY spin chain subject to a constant homogeneous magnetic field and to a single mode of quantized electromagnetic field. The respective interaction is described by the Zeeman term which couples the spin magnetic moments to the magnetic fields. Instead of a spin chain one can think of a XY system of interacting two-level atoms and a Stark term describing the interaction between the atomic electric dipole moments and the electric component of the mode. Then the formal Hamiltonian does not change, which makes the obtained results applicable to both types of problems. Here, we do not account for decoherence mechanisms, that is we deal with a closed system that does not interact with the outside world. Hamiltonian of our system may be written down as the sum of the quantized free electromagnetic field, the XY model and the Dicke Hamiltonian. Applying the Rotating Wave Approximation to the Dicke Hamiltonian we explored the dynamics of the model depending upon the relevant parameters. This allowed us to find the domain of validity of studies based on the XY interaction in empir-

* boradjiev@issp.bas.bg

ical models [23–26]. The model under consideration may find applications in problems related to a bosonic mode in a spin-bath, spin chains or linear molecular aggregates in a single-mode cavity, and in the study of superradiant and superabsorbing systems.

The rest of the paper is organized as follows. We proceed with the description of the model in Section II. Section III is devoted to the conditions for validity and application of RWA. In Sec. IV the model Hamiltonian is transformed to the fermion basis diagonalizing the XY chain part. Some notations and definitions are given in Sec. V. In Sec. VI the exact analytical solution for the single excitation case is derived. Section VII deals with the formal solution for the general (multiple excitation) case. Also, the results from numerical simulations in the large detuning regime, given that at the beginning all the excitations are in the field, are presented. In Sec. VIII effective Hamiltonians approximating the Hamiltonian under consideration are obtained. In Sec. IX the evolution of the system, when all the excitations are contained in the spin chain at the beginning, is considered. The summary of the results is given in Sec. X. There are two appendices. In Appendix A we present the detailed calculation of the conditions for the RWA. In Appendix B we recall the diagonalization procedure for the XY spin chain model, discuss its ground state, and derive the full Hamiltonian in the respective basis.

II. THE MODEL

The Hamiltonian of a chain of interacting (effective) spins, placed in a magnetic field reads

$$\hat{H} = \hat{H}^{FF} + \hat{H}^{SM} + \hat{V}, \quad (1)$$

where, assuming that the component of the magnetic field along z -direction is time independent, the quantized free electromagnetic field Hamiltonian \hat{H}^{FF} is given by

$$\hat{H}^{FF} = \hbar\omega(\hat{n}_x + \hat{n}_y), \quad (2)$$

where \hat{n}_x and \hat{n}_y are the number operators for the x and y polarized components of the magnetic field, and ω is the frequency of the field. Here we skip the zero point energy.

In (1), the Hamiltonian, describing the interacting spin system is given by the XY spin model [27, 28]

$$\hat{H}^{SM} = \hat{H}^{XY} = 2J \sum_{i>j} (\hat{S}_{ix}\hat{S}_{jx} + \hat{S}_{iy}\hat{S}_{jy}), \quad (3)$$

where J is a coupling constant and \hat{S}_i are dimensionless spin- $\frac{1}{2}$ (pseudo-)vector operators, whose components obey the following commutation relations

$$[\hat{S}_{i\eta}, \hat{S}_{j\zeta}] = i\delta_{ij}\varepsilon_{\eta\zeta\theta}\hat{S}_{i\theta}, \quad \eta, \zeta, \theta = x, y, z, \quad (4)$$

with i, j labeling the sites.

The remaining part of (1) is given by

$$\hat{V} = - \sum_i \hat{\mu}_{S_i} \cdot \hat{\mathbf{B}} \quad (5)$$

where we define the magnetic field $\hat{\mathbf{B}}$, and the interaction between $\hat{\mathbf{B}}$ and the magnetic moments $\hat{\mu}_{S_i}$ associated with the spins in the XY model.

To proceed further, we use the relation between the magnetic moments and the spins, i.e. $\hat{\mu}_{S_i} = -2\mu\hat{\mathbf{S}}_i$, where μ is the Bohr magneton. Moreover, we assume that the constant homogeneous magnetic field is applied along the z -direction and a quantized electromagnetic mode with wave vector along z -axis interacts with a number p of spin magnetic moments only (the effect of the electric component of the field is neglected). Moreover, we suppose that the spin chain resides in the (x, y) plane, and therefore, it is reasonable to work in the dipole approximation ($e^{\pm i\mathbf{k}z} \approx 1$). For convenience we depicted schematically the system in Fig. 1. With the above assumptions we can write the interaction term as

$$\hat{V} = \hbar\omega_1 \sum_i \hat{S}_{iz} + i\hbar\Omega \sum_{i=1}^p [\hat{S}_{iy}(\hat{a}_x - \hat{a}_x^\dagger) - \hat{S}_{ix}(\hat{a}_y - \hat{a}_y^\dagger)]. \quad (6)$$

Here $\hat{a}_{x,y}$ and $\hat{a}_{x,y}^\dagger$ are the annihilation and creation operators for the linearly polarized field, Ω parametrizes the coupling between the spins and the circularly polarized magnetic field, and ω_1 parameterizes the coupling between the spins and the constant component of the magnetic field. Note that if the sum in the first term runs over $1 \leq i \leq p$, then \hat{V} would coincide with the Dicke model [15].

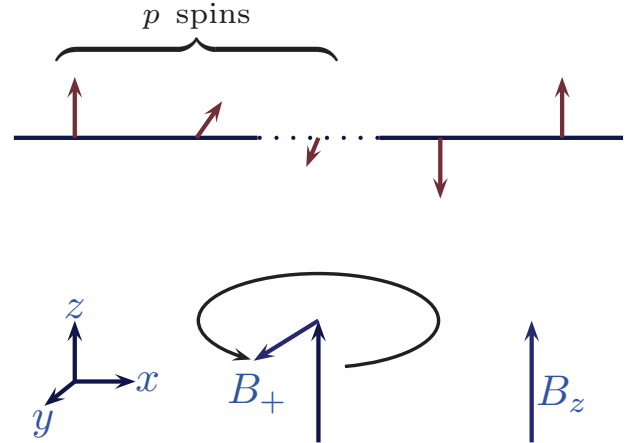


FIG. 1. (Color online) Setup of the model. B_+ and B_z are the left circularly polarized and constant components of the magnetic field respectively and the tilted arrows in the upper part of the diagram represent the spin chain. The right circularly polarized component of the field is not shown in the figure since we discard it by means of the RWA, see Sec. III.

Because of the specificity of the problem it will be more convenient to introduce a set of creation and annihilation operators for circularly polarized field defined via

$$\hat{a}_{\pm} = \mp \frac{1}{\sqrt{2}}(\hat{a}_x \mp i\hat{a}_y), \quad (7)$$

with the following canonical commutators

$$[\hat{a}_\eta, \hat{a}_\zeta] = [\hat{a}_\eta^\dagger, \hat{a}_\zeta^\dagger] = 0, \quad [\hat{a}_\eta, \hat{a}_\zeta^\dagger] = \delta_{\eta\zeta}, \quad \eta, \zeta = +, -, \quad (8)$$

and the spin ladder operators

$$\hat{S}_{i\pm} = \hat{S}_{ix} \pm i\hat{S}_{iy}, \quad \hat{S}_{iz} = \hat{S}_{iz}, \quad (9)$$

that satisfy the commutation relations

$$[\hat{S}_{i+}, \hat{S}_{j-}] = 2\delta_{ij}\hat{S}_{iz}, \quad [\hat{S}_{iz}, \hat{S}_{j\pm}] = \pm\delta_{ij}\hat{S}_{i\pm}. \quad (10)$$

In terms of the operators (7) and (9), Hamiltonian (1) takes the form

$$\hat{H} = \hbar\omega \left(\hat{n}_+ + \hat{n}_- + \frac{p}{2} + \sum_{i=1}^p \hat{S}_{iz} \right) + J \sum_{i>j} (\hat{S}_{i+}\hat{S}_{j-} + \hat{S}_{i-}\hat{S}_{j+}) + \hat{H}^D, \quad (11a)$$

with

$$\hat{H}^D = \hbar\omega_1 \sum_{i>p} \hat{S}_{iz} + \hbar\Delta \sum_{i=1}^p \hat{S}_{iz} - \frac{\hbar\Omega}{\sqrt{2}} \sum_{i=1}^p \left[(\hat{a}_+ + \hat{a}_-^\dagger)\hat{S}_{i+} + (\hat{a}_- + \hat{a}_+^\dagger)\hat{S}_{i-} \right], \quad (11b)$$

where we define the detuning $\Delta = \omega_1 - \omega$ and the number operators $\hat{n}_\pm = \hat{a}_\pm^\dagger \hat{a}_\pm$. In (11), and from now on, we explicitly consider only this part of the chain with sites $i > 1$. The terms involving sites with $i \leq 0$ can be treated analogously. Moreover, note that we add $\frac{p}{2}\hbar\omega$ to the Hamiltonian in order to obtain the correct number of excitations operator.

III. ROTATING WAVE APPROXIMATION

The essence of RWA consists in neglecting corrections that are inversely proportional to the frequency ω and its higher degrees in the solution of the Schrödinger equation. In problems, like Jaynes-Cummings model [13], it is usually assumed that the field is tuned near resonance, so that the detuning $\Delta = \omega_1 - \omega$ is orders of magnitude smaller than $\omega_1 + \omega \sim 2\omega$, the interaction constant Ω is much smaller than the photon frequency so $\alpha\Omega \ll \omega$, $\alpha \approx \sqrt{n}$, and the time of the process is much longer than the period of the field $T \gg 2\pi/\omega$. For its p -spin generalization – the Tavis-Cummings model – one of the conditions needs to be modified, namely

$$p \frac{\alpha_- \Omega}{\omega} \ll 1, \quad \frac{\alpha_+ \Omega}{\omega} \ll 1, \quad \alpha_\pm \approx \sqrt{n_\pm}. \quad (12)$$

The condition (12) is best fulfilled in the case of left circularly polarized field-mode. This is exactly what we will be concerned with in the following. Then the right circularly polarized photons may appear only due to the counter-rotating terms, and hence, $\alpha_- \leq 1$. For the Dickie part (11b)

of the Hamiltonian \hat{H} (11a) with $J \neq 0$, we find that the RWA can be applied provided also that

$$\frac{JT}{\hbar} \ll 1. \quad (13)$$

The above follows from the requirement of the convergence of some perturbation series. More rigorous calculations might lead to a less restrictive requirement.

Furthermore, we find that the same conditions, $T \gg 2\pi/\omega$ and (12,13), are sufficient to ensure the validity of the RWA for the Dicke part of \hat{H} (11a) in the large detuning regime ($\Delta \rightarrow -\omega$) as well.

We would like to keep the XY terms unaltered when performing RWA. To this end we need one more sufficient condition

$$p \frac{JT}{\hbar} \ll 1, \quad \text{for } \Delta \rightarrow 0, \quad (14a)$$

$$p \frac{J}{\hbar\omega} \lesssim 1, \quad \text{for } \Delta \rightarrow -\omega, \quad (14b)$$

and to consider the XY chain in the nearest-neighbor approximation placed in a cavity. The latter guarantees that all the spins interact with the photon mode. Due to the very restrictive condition (14a) we will concentrate our efforts mainly on the large detuning regime. More details and the sketch of the proof of the above estimates is outlined in Appendix A.

In the framework of RWA there are a couple of important consequences, that help us simplify Hamiltonian (11): First, we neglect any term containing right-hand circularly polarized components of the field that do not conserve the energy, such as $\hat{a}_-^\dagger \hat{S}_{i+}$ and $\hat{a}_- \hat{S}_{i-}$, and we set $\hat{n}_- = 0$. Second, since the number of excitations operator \hat{N} commutes with the ensuing approximated Hamiltonian, it is an invariant quantity (a constant of motion).

With the above simplifications, apart from the constant $\hbar\omega\hat{N}$, the Hamiltonian of the XY chain interacting with the photon mode splits into the sum of two parts: The Tavis-Cummings Hamiltonian \hat{H}^{TC} [14] and the XY spin Hamiltonian $\hat{H}_{<p}^{XY}$ [27–29], that are well known exactly solvable models. That is

$$\hat{H} = \hbar\omega\hat{N} + \hat{H}_{<p}^{XY} + \hat{H}^{TC}, \quad (15a)$$

where

$$\hat{N} = \left(\hat{n}_+ + \frac{p}{2} + \sum_{i=1}^p \hat{S}_{iz} \right), \quad (15b)$$

$$\hat{H}_{<p}^{XY} = J \sum_{p \geq i > j} (\hat{S}_{i+}\hat{S}_{j-} + \hat{S}_{i-}\hat{S}_{j+}), \quad (15c)$$

$$\hat{H}^{TC} = \hbar\Delta \sum_{i=1}^p \hat{S}_{iz} - \frac{\hbar\Omega}{\sqrt{2}} \sum_{i=1}^p (\hat{a}_+ \hat{S}_{i+} + \hat{a}_+^\dagger \hat{S}_{i-}). \quad (15d)$$

Henceforth we omit the “+” subscript on the photon creation and annihilation operators and will not be worried too much about the fulfillment of the conditions for the validity of RWA. The main goal will be to make the dependencies on the parameters more lucid.

IV. DIAGONALIZATION OF XY PART OF THE HAMILTONIAN

To be more specific, here and below, we consider the periodic XY model in the nearest-neighbor approximation, and we assume an even number of sites p . Note, that the periodic boundary conditions, $\hat{S}_{p+1\pm} = \hat{S}_{1\pm}$, imply that the upper bound of the double sum in the XY Hamiltonian (15c) must be changed from $i = p, j = p - 1$ to $i = p + 1, j = p$.

In order to analyze the Schrödinger equation with Hamil-

tonian (15), we transform \hat{H} so that \hat{H}^{XY} may be diagonalized [23, 25, 29]. The diagonalization procedure is outlined in Appendix B 1. This yields

$$\hat{H} = \hbar\omega\hat{N} + \hat{H}(J, \Delta) - \frac{\hbar\Omega}{\sqrt{2}} \sum_{i=1}^p \left(\hat{a}\hat{S}_{i+} + \hat{a}^\dagger\hat{S}_{i-} \right), \quad (16a)$$

with

$$\hat{H}(J, \Delta) = \sum_{\sigma=\pm} \frac{1+\sigma P}{2} \left\{ \sum_{k \in BZ} (2J\Lambda_{k\sigma} + \hbar\Delta) \left(\hat{\eta}_{k\sigma}^\dagger \hat{\eta}_{k\sigma} - \frac{1}{2} \right) \right\} \frac{1+\sigma P}{2} \quad \text{and} \quad (16b)$$

$$\sum_{i=1}^p \hat{S}_{i+} = \sum_{\sigma=\pm} \frac{1+\sigma P}{2} \sum_{k \in BZ} \hat{\eta}_{k\sigma}^\dagger \sum_{i=1}^p \phi_{ki}^{(\sigma)*} \exp \left(i\pi \sum_{q, q' \in BZ} \sum_{j=1}^{i-1} \phi_{qj}^{(\sigma)*} \phi_{q'j}^{(\sigma)} \hat{\eta}_{q\sigma}^\dagger \hat{\eta}_{q'\sigma} \right) \frac{1-\sigma P}{2}, \quad (16c)$$

where $\hat{\eta}_{k\sigma}$ and $\hat{\eta}_{k\sigma}^\dagger$ are Fermi operators obeying the canonical anti-commutation relations

$$\{\hat{\eta}_{k\sigma}, \hat{\eta}_{k'\sigma'}^\dagger\} = \delta_{kk'}, \quad \{\hat{\eta}_{k\sigma}, \hat{\eta}_{k'\sigma'}\} = \{\hat{\eta}_{k\sigma}^\dagger, \hat{\eta}_{k'\sigma'}^\dagger\} = 0, \quad (17)$$

ϕ_{ki}^σ are components of the orthonormal vectors ϕ_k^σ ,

$$\phi_{kj}^\sigma = \frac{1}{\sqrt{p}} e^{ik^\sigma j}, \quad \sum_{i=1}^p \phi_{ki}^\sigma \phi_{k'i}^{\sigma*} = \delta_{kk'}, \quad (18)$$

the energies (in units of $2J$) $\Lambda_{k\sigma}$ for the free XY model read

$$\Lambda_{k\sigma} = \cos(k^\sigma), \quad (19)$$

and the quasi-momenta summations run over the p discrete values in the Brillouin zone (BZ)

$$k_\eta^\sigma = -\pi + \left(2\eta + \frac{\sigma-3}{2} \right) \frac{\pi}{p}, \quad \eta = 1, 2, \dots, p. \quad (20)$$

The lower index in quasi-momentum is omitted everywhere except in cases of summation over η in Sec. VII A.

V. BASIS AND PHYSICAL QUANTITIES

In this Section we define the basis in which we will further write the matrix form of the Schrödinger equation and define the relevant physical quantities for the description of the dynamics of the system.

A. Basis states

We consider the regime of strong magnetic field B_z , quantified by the condition $\hbar\omega_1 \geq 2J$, when the ground state of the XY model interacting with B_z is the free of η -quasi-particles (ferromagnetic) state, see Appendix B 2 a. Assuming that at the beginning of the process the excitations of the

system are contained in the photon field and that the XY model subject to B_z field is in its ground state, we define the initial state to be the $(p+1)$ -dimensional product state

$$|N; 0\rangle \equiv |N\rangle \otimes |0\rangle, \quad |0\rangle \equiv |0, 0, \dots, 0\rangle, \quad (21)$$

where N and 0's stand for the photon and η_k 's occupation numbers, respectively.

Henceforth, we will also use the following shorthand notation [30]

$$|\vec{\eta}_m\rangle = \prod_{l=1}^m \hat{\eta}_{\eta_l \sigma_m}^\dagger |0\rangle = \hat{\eta}_{\eta_1 \sigma_m}^\dagger \hat{\eta}_{\eta_2 \sigma_m}^\dagger \hat{\eta}_{\eta_3 \sigma_m}^\dagger \dots \hat{\eta}_{\eta_m \sigma_m}^\dagger |0\rangle, \quad (22a)$$

$$\vec{\eta}_m \equiv (\eta_1, \eta_2, \dots, \eta_m), \quad 1 \leq \eta_1 < \eta_2 < \dots < \eta_m \leq p \quad (22b)$$

for the eigenstates of the XY chain.

The number of excitations N is a conserved quantity, determined by the initial state. So the dynamics of the system is restricted to the $D_{p,N}$ -dimensional,

$$D_{p,N} = \sum_{m=0}^{\min\{N,p\}} C_p^m, \quad C_p^m = \frac{p!}{m!(p-m)!}, \quad (23)$$

subspace of the Hilbert space (N -sector) spanned by the basis states

$$\{|N-m; \vec{\eta}_m\rangle\}. \quad (24)$$

Obviously, here m stands for the number of excitations in the XY -chain.

An arbitrary state in the N -sector can be always given by the expansion

$$|\psi_N(t)\rangle = \sum_{m=0}^{\min\{N,p\}} \sum_{\vec{\eta}_m} A_{\vec{\eta}_m}^m(t) |N-m; \vec{\eta}_m\rangle, \quad (25)$$

where $A_{\vec{\eta}_m}^m(t)$ are time-dependent probability amplitudes.

B. Physical quantities

We are interested in the influence of the spin chain on the field and vice versa. Nonetheless, we are not interested in the probability for the specific state of the chain but rather in the expectation values of operators corresponding to relevant physical quantities. Therefore, to describe the evolution of the system in state $|\psi_N(t)\rangle$, as in Refs. [22, 25], we consider the reduced photon occupation number

$$P_{\text{ph}}(t) = \frac{\langle \psi_N(t) | \hat{n} | \psi_N(t) \rangle}{N} = \sum_{m=0}^N \sum_{\vec{\eta}_m} \left(1 - \frac{m}{N}\right) P_{\vec{\eta}_m}^m(t), \quad (26)$$

$$P_{\vec{\eta}_m}^m(t) = |A_{\vec{\eta}_m}^m(t)|^2, \quad (27)$$

and in addition, the (dimensionless) magnetization per site of the XY spin chain

$$m(t) = \frac{M(t)}{\mu p} = -\frac{2}{p} \langle \psi_N(t) | \sum_{i=1}^p \hat{S}_{iz} | \psi_N(t) \rangle = 1 - \frac{2NP_m(t)}{p}, \quad (28)$$

$$P_m(t) = 1 - P_{\text{ph}}(t). \quad (29)$$

Note that Eq. (28) is the result of the invariance of the number of excitations operator Eq. (15b), which also implies that $P_{\text{ph}}(t)$, $m(t)$, and p/N are not independent quantities.

VI. SINGLE EXCITATION

The case of a single excitation in the system is of peculiar interest since its solution can be obtained in a closed form. Moreover, this result will set the basis for our further considerations.

As we start from the initial state (21) with $N = 1$, the dynamics of the system is restricted to the states describing single excitations. The only possibly non-vanishing transition matrix elements of Hamiltonian (16) are

$$\langle 1_k; 0 | \hat{H} | 1; 0 \rangle \equiv \langle 0, \dots, 1_k, \dots, 0 | \hat{H} | 1; 0, \dots, 0_k, \dots, 0 \rangle, \quad \forall k \in BZ, \quad (30)$$

and their Hermitian conjugates. The exponents in (16c) are effectively unity for these transitions. Thus they can be replaced by mathematically identical (effectively unit) Jordan-Wigner string operators [31],

$$\exp\left(\pm i\pi \sum_{q, q' \in BZ} \sum_{j=1}^{i-1} \phi_{qj}^* \phi_{q'j} \hat{\eta}_q^\dagger \hat{\eta}_{q'}\right) \rightarrow \exp\left(\pm i\pi \sum_{q=-\pi}^{k-2\pi/p} \hat{\eta}_q^\dagger \hat{\eta}_q\right). \quad (31)$$

Then by means of Jordan-Wigner transformations we define a set of half-spin operators

$$\hat{\Sigma}_{k-} = \exp\left(-i\pi \sum_{q=-\pi}^{q=k-2\pi/p} \hat{\eta}_q^\dagger \hat{\eta}_q\right) \hat{\eta}_k, \quad (32a)$$

$$\hat{\Sigma}_{k+} = \hat{\eta}_k^\dagger \exp\left(i\pi \sum_{q=-\pi}^{q=k-2\pi/p} \hat{\eta}_q^\dagger \hat{\eta}_q\right), \quad (32b)$$

$$\hat{\Sigma}_{kz} = \hat{\eta}_k^\dagger \hat{\eta}_k - \frac{1}{2}, \quad (32c)$$

obeying the following commutation relations

$$[\hat{\Sigma}_{q+}, \hat{\Sigma}_{q'-}] = 2\delta_{qq'} \hat{\Sigma}_{qz}, \quad [\hat{\Sigma}_{qz}, \hat{\Sigma}_{q'\pm}] = \pm \delta_{qq'} \hat{\Sigma}_{q\pm}. \quad (33)$$

With the aid of these operator variables we can rewrite Hamiltonian (16) in the following form

$$\hat{H} = \hbar\omega \hat{N} + \sum_{k \in BZ, k \neq 0} P_k \hat{\Sigma}_{kz} + \hat{H}_{JC}, \quad (34a)$$

with

$$\hat{H}_{JC} = P_0 \hat{\Sigma}_{0z} + \frac{Q}{2} (\hat{a} \hat{\Sigma}_{0+} + \hat{a}^\dagger \hat{\Sigma}_{0-}), \quad (34b)$$

and

$$P_k = 2J\Lambda_k + \hbar\Delta, \quad Q = -\hbar\Omega\sqrt{2p}. \quad (34c)$$

In (34a), we have used the relation

$$\sum_{i=1}^p \phi_{ki} = \sqrt{p} \delta_{k0}, \quad (35)$$

which is a direct consequence of the orthogonality condition (18).

Apart from the operator \hat{N} , Hamiltonian (34a) consists of two additional terms $-\sum_{k \in BZ, k \neq 0} P_k \hat{\Sigma}_{kz}$ and \hat{H}_{JC} . The first one is also a constant of motion

$$\left[\sum_{k \in BZ, k \neq 0} P_k \hat{\Sigma}_{kz}, \hat{H} \right] = 0, \quad (36)$$

that describes the free evolution of two-level systems with excitation energies P_k . The second term, i.e. \hat{H}_{JC} given explicitly in (34b), describes the field-induced dynamics of the XY system. It corresponds to the Jaynes-Cummings model for a two-level system interacting with a single-mode quantized cavity field.

Since only the zero-momentum mode is involved in the interaction described by (34b), the dynamics is confined to the two-dimensional subspace

$$\{|\Phi_{\text{in}}\rangle, |0; \frac{1}{2}_0\rangle\}, \quad (37a)$$

with

$$|\Phi_{\text{in}}\rangle \equiv |1; -\frac{1}{2}\rangle \equiv |1; -\frac{1}{2}, -\frac{1}{2}, \dots, -\frac{1}{2}\rangle, \quad (37b)$$

$$|0; \frac{1}{2}_0\rangle \equiv |0; -\frac{1}{2}, -\frac{1}{2}, \dots, \frac{1}{2}_{k=0}, \dots, -\frac{1}{2}\rangle, \quad (37c)$$

where the spin chain subsystem is contained in the Σ -representation.

The solution of the Schrödinger equation with Hamiltonian \hat{H}_{JC} (34b) and initial condition $|\Phi_{\text{in}}\rangle$ (37b) reads [13]

$$|\Phi(t)\rangle = -i \sin\left(\frac{\mathcal{E}_+ t}{\hbar}\right) \sin(\phi) |0; \frac{1}{2}_0\rangle + \left[i \sin\left(\frac{\mathcal{E}_+ t}{\hbar}\right) \cos(\phi) + \cos\left(\frac{\mathcal{E}_+ t}{\hbar}\right) \right] |1; -\frac{1}{2}\rangle, \quad (38)$$

where the angle ϕ and the eigenvalues \mathcal{E}_\pm are given by

$$\phi = \tan^{-1}\left(\frac{Q}{P_0}\right), \quad (39a)$$

$$\mathcal{E}_\pm = \pm \frac{1}{2} \sqrt{P_0^2 + Q^2}. \quad (39b)$$

We can now write down the solution of the problem of interest, namely the solution of the Schrödinger equation with Hamiltonian (34a) and initial condition

$$|\psi_{\text{in}}\rangle \equiv |1; -\frac{1}{2}, -\frac{1}{2}, \dots, -\frac{1}{2}\rangle. \quad (40)$$

The solution is obtained by recovering the constants that add up to the phase

$$\begin{aligned} |\psi\rangle &= \exp\left(-\frac{it}{\hbar} \hat{H}\right) |\psi_{\text{in}}\rangle \\ &= \exp\left\{-\frac{it}{\hbar} \left[\frac{P_0}{2} - \sum_{k \in BZ} \frac{P_k}{2} + \hbar\omega \left(1 - \frac{p}{2}\right)\right]\right\} |\Phi(t)\rangle. \end{aligned} \quad (41)$$

Note that the initial condition $|\psi_{\text{in}}\rangle$ takes the same form as $|\Phi_{\text{in}}\rangle$. To avoid any confusion, we remind that the former is related to a real-space configuration in the spin representation (where \hat{S}_i operate), while the latter is related to a momentum space configuration in the spin Σ -representation (where $\hat{\Sigma}_k$ operate). Since both reflect the same physical state, though in different bases, we have $|\psi_{\text{in}}\rangle \equiv |\Phi_{\text{in}}\rangle$.

From (38) we have for the time-dependent probabilities of the excitation in the zero-momentum mode and in the field-boson, respectively,

$$\begin{aligned} P_{m0}(t) &= \langle \Phi(t) | \left(\hat{\Sigma}_{0z} + \frac{1}{2} \right) | \Phi(t) \rangle \\ &= \frac{Q^2}{P_0^2 + Q^2} \sin^2\left(\frac{\mathcal{E}_+ t}{\hbar}\right), \end{aligned} \quad (42)$$

$$P_{\text{ph}}(t) = 1 - P_{m0}(t). \quad (43)$$

The probabilities oscillate, reflecting the transfer of excitation between the field and the spin chain, with frequency \mathcal{E}_+/\hbar , and an amplitude determined by the angle ϕ . It is clear, see the definitions (39), that with an increase of the absolute value of the detuning $|P_0|$ the amplitude of the oscillation decreases while its frequency increases. Obviously, the magnetization per site (28) also has oscillatory behavior.

A remark concerning the range of validity of the results in the large detuning regime is in order. The amplitude of the oscillation depends on the ratio $Q/P_0 \sim \sqrt{2p}\Omega/\Delta$, combined with the RWA condition $p\Omega/\Delta \ll 1$ leads to the requirement $Q/P_0 \ll \sqrt{2/p}$. The latter puts an upper bound on Q/P_0 for which our considerations are valid. The bound increases as the number of spins p decreases and thus the amplitude of the oscillations of $P_{\text{ph}}(t)$ and the magnetization $m(t)$ might become larger within RWA.

An example of dynamics of the probabilities for an excitation is plotted in Fig. 2. Two cases are considered – anti-ferromagnetic ($J > 0$) and ferromagnetic ($J < 0$). Due to the larger absolute value of the detuning $|P_0|$, the amplitude is smaller and the frequency is higher in the case

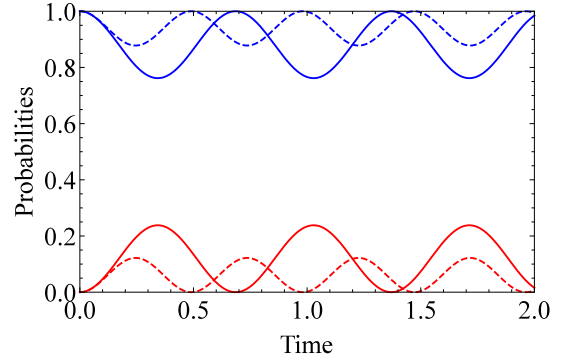


FIG. 2. (Color online) Dynamics of the probabilities for an excitation in the field, $P_{\text{ph}}(t)$, blue curves, and in the zero-momentum mode, $P_m(t)$, red curves, for a chain of $p = 10$ spins and $N = 1$ excitation. The coupling J and the detuning (in units of $\tau = 1/|\Omega|$) are $J\tau/\hbar = 1$ and $\Delta\tau = -10$, respectively. The solid curves correspond to the anti-ferromagnetic case ($J > 0$), and the dashed curves to the ferromagnetic case ($J < 0$). The dimensionless time t/τ is plotted on the abscissa.

of a ferromagnetic spin chain. The physical reason to have larger $|P_0|$ is that the energy $-2|J|\Lambda_0$ of the zero-momentum mode in the ferromagnetic XY chain is lower. Even for the anti-ferromagnetic chain, the reduction of the magnetization does not exceed 5%, for this specific choice of parameters.

VII. GENERAL (MULTIPLE EXCITATION) CASE

Here we recall the explicit form of the Hamiltonian matrix elements and the formal solution of the problem, which are then used for the numerical computations.

A. Formal solution

Here we turn our attention to the general case of multiple excitations, when the number of excitations does not exceed the number of spins, $N \leq p$.

In this case, up to an irrelevant constant, the matrix elements of Hamiltonian (16) are given by [32]

$$\begin{aligned} &\langle \vec{\eta}'_{m'}; N - m' | \hat{H} | N - m; \vec{\eta}_m \rangle \\ &= \delta_{mm'} \prod_{l=1}^m \delta_{\eta'_l \eta_l} [\mathcal{E}_{\vec{\eta}_m} + \hbar\omega(N - m)] \\ &\quad - \delta_{m'm+1} \frac{\hbar\Omega}{\sqrt{2}} F_{\vec{\eta}'_{m+1} \vec{\eta}_m}^* \sqrt{N - m} \\ &\quad - \delta_{m'm-1} \frac{\hbar\Omega}{\sqrt{2}} F_{\vec{\eta}_m \vec{\eta}'_{m-1}} \sqrt{N - m + 1}. \end{aligned} \quad (44)$$

With $\mathcal{E}_{\vec{\eta}_m}$ is the total energy of the m excitations of the XY

chain in the state $|\vec{\eta}_m\rangle$,

$$\mathcal{E}_{\vec{\eta}_m} = \sum_{l=1}^m \varepsilon_{\eta_l}, \quad \varepsilon_{\eta} = \hbar\omega_1 + 2J\Lambda_{k_{\eta}}, \quad (45)$$

$F_{\vec{\eta}_{n+1}\vec{\eta}'_n}$ is the collective spin operator matrix element,

$$\begin{aligned} F_{\vec{\eta}_{n+1}\vec{\eta}'_n} &\equiv \langle \vec{\eta}'_n | \sum_{j=1}^p \hat{S}_{j-} | \vec{\eta}_{n+1} \rangle \\ &= 2^n p^{\frac{1}{2}-n} \delta(\Delta_{\vec{\eta}_{n+1}, \vec{\eta}'_n}, 0) h_{\vec{\eta}_{n+1}, \vec{\eta}'_n}, \end{aligned} \quad (46)$$

where

$$\delta(x, y) = \begin{cases} 1 & \text{if } x - y = 2\pi r, \quad r \in \mathbb{Z}, \\ 0 & \text{otherwise,} \end{cases} \quad (47)$$

is the Kronecker delta function,

$$\Delta_{\vec{\eta}_{n+1}, \vec{\eta}'_n} = \sum_{j=1}^{n+1} k_{\eta_j}^{\sigma_{n+1}} - \sum_{i=1}^n k_{\eta'_i}^{\sigma_n} \quad (48)$$

is the momentum transfer between the corresponding states, and

$$h_{\vec{\eta}_{n+1}, \vec{\eta}'_n} = \frac{\prod_{i>i'} \left(e^{-ik_{\eta'_i}^{\sigma_n}} - e^{-ik_{\eta'_i}^{\sigma_n}} \right) \prod_{j>j'} \left(e^{ik_{\eta_j}^{\sigma_{n+1}}} - e^{ik_{\eta_j}^{\sigma_{n+1}}} \right)}{\prod_{i=1}^n \prod_{j=1}^{n+1} \left[1 - e^{-i(k_{\eta_j}^{\sigma_{n+1}} - k_{\eta'_i}^{\sigma_n})} \right]}. \quad (49)$$

Note, that for non-vanishing off-diagonal matrix elements the number of η -excitations can only differ by one.

With this at hand, for any N -sector, we can write the Schrödinger equation in matrix form in the basis $\{|N - m; \vec{\eta}_m\rangle\}$, and integrate it to find the probability amplitudes $A(t)$. Formally, we have

$$A(t) = \exp\left(-\frac{it}{\hbar} H\right) A_{\text{in}}, \quad A_{\text{in}} = (1, 0, 0, \dots, 0)^T. \quad (50)$$

B. Numerical results

The dynamics of the reduced photon number $P_{\text{ph}}(t)$ and magnetization per site $m(t)$ for various values of the number of spins p , total number of excitations N , and detuning Δ , is shown in Fig. 3. Particular cases near resonance $\Delta\tau \ll 1$ ($\tau = 1/|\Omega|$) are not considered here, while the on-resonance regimes will be discussed in Sec. IX. In this Section we explore the regime of large detuning $\Delta\tau \gg 1$.

As a general remark we see that Fig. 3 reveals an oscillatory behavior of $P_{\text{ph}}(t)$ and $m(t)$ with frequency slightly dependent on the values of p and N . In fact, the frequency depends mostly on Δ and J , for fixed coupling Ω .

In Fig. 3 a) several curves represent the behavior of $P_{\text{ph}}(t)$ for different values of p and N , at fixed ratio p/N . With the increase of their values the amplitude also increases,

because the larger part of the excitations is exchanged between the field and the chain. The curves in Fig. 3 b) represent the magnetization $m(t)$ for the same set of values p and N as in Fig. 3 a). The figure is completely analogous to Fig. 3 a), that follows from (28), where for $p/N = 2$ we obtain $P_{\text{ph}}(t) = m(t)$.

The dynamics of $P_{\text{ph}}(t)$ for different values of N and fixed p is shown in Fig. 3 c). We observe that the amplitude of $P_{\text{ph}}(t)$ is almost independent on N . In Fig. 3 d) the dynamics of the respective magnetization $m(t)$ is shown. Contrary to the $P_{\text{ph}}(t)$, the amplitude of $m(t)$ is increasing against N . We see exactly the opposite behavior in Figs. 3 e) and 3 f) where the dynamics of $P_{\text{ph}}(t)$ and $m(t)$ are shown for different values of p and fixed N . This can be understood from the expression (28) that shows a symmetry with respect to simultaneous exchange of $P_{\text{ph}}(t)$ and $m(t)$ together with p and $2N$.

In Figs. 3 g) and 3 h) we observe an oscillatory behavior where the frequency of both $P_{\text{ph}}(t)$ and $m(t)$ is increasing, while their amplitudes are decreasing, with the increase of the absolute value of the detuning.

The dependence of $P_{\text{ph}}(t)$ on J when J is not a small quantity, though we assume so throughout the paper, is shown for completeness in Fig. 4. Both the amplitude and frequency depend in a nontrivial manner on J . The behavior of the magnetization $m(t)$ (not shown in the figure) is qualitatively the same as for $P_{\text{ph}}(t)$.

VIII. EFFECTIVE HAMILTONIANS

In this Section we sketch how one can in principle develop (time-independent) perturbation theory for the interacting XY -model (16) in the large detuning regime, given that initially all the excitations are contained in the field. We have verified numerically that the found effective Hamiltonians are less precise in the near resonant case.

We showed in the single-excitation case, Sec. VI, that the excitation is *shared* among the field and the zero-momentum mode of the chain. In the case of multiple excitations, a close inspection of the transition matrix elements in (44), similarly, leads us to the conjecture that the majority of excitations are shared between the chain modes of zero net momentum and the field. Applying this conjecture, we will be able to identify two somehow different perturbative expansions. These are of the form of the expansions of the perturbed tridiagonal Hamiltonian matrix model and of the perturbed Tavis-Cummings model. We will use only the unperturbed Hamiltonians, and will regard them as reference effective Hamiltonians reproducing approximately the short-time evolution in the case of small number of total excitations. The reason not to deal with the correction terms is that they are not given by simple analytic formulas. Depending on the accuracy that is needed, at some point it may become much more practical merely to run a full numerical simulation.

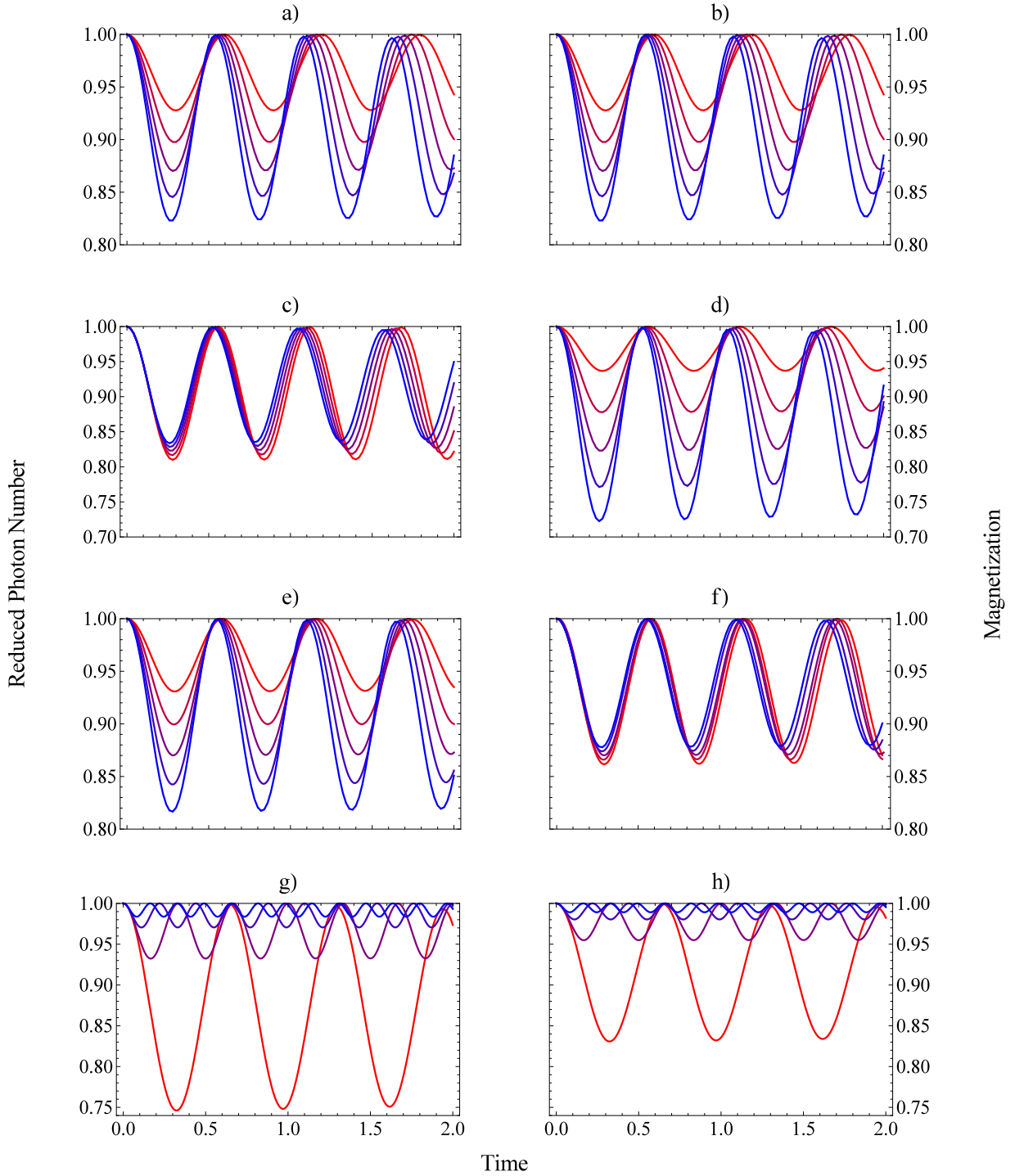


FIG. 3. (Color online) Dynamics of the reduced photon occupation number $P_{\text{ph}}(t)$ (left panel) and (dimensionless) magnetization per site $m(t)$ (right panel) for various values of the control parameters. In Figs. a), and b), both the number of excitations and the number of the spins in the chain are varied simultaneously $(N, p) = (2, 4), (3, 6), \dots (6, 12)$, keeping the ratio $p/N = 2$ fixed. The values of the other parameters are $J\tau/\hbar = 1$, $\Delta\tau = -12$. In Figs. c), and d), the number of excitations is varied in the range $N = 2, 4, \dots 10$. We choose $p = 12$ and the values of the parameters are the same as for the ones for Figs. a) and b). In Figs. e), and f), the number of spins in the chain takes the values $p = 4, 6, \dots 12$. We choose $N = 4$ and the values of the parameters are the same as for the ones for Figs. a) and b). In Figs. g), h) the detuning varies in the range $\Delta\tau = -10, -20, -30, -40$ and the values of the other parameters are $N = 4$, $p = 12$, $J\tau/\hbar = 1$. The increase of the absolute value of the components varied is coded with a change of the color from red to blue. The dimensionless time t/τ is plotted on the abscissas.

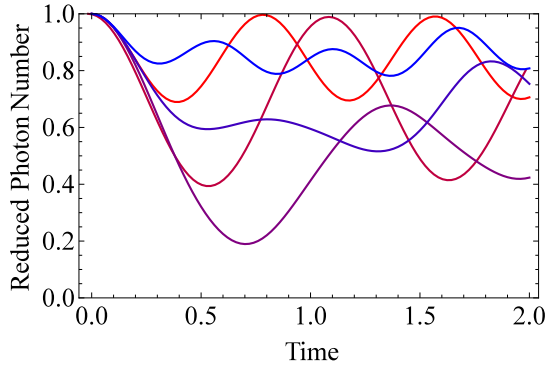


FIG. 4. (Color online) Dynamics of the reduced photon occupation number $P_{\text{ph}}(t)$ for $N = 4, p = 10, \Delta\tau = -10$, and various values of the spin-spin coupling $J\tau/\hbar = 2, 4, \dots, 10$. The dimensionless time t/τ is plotted on the abscissa. The increase of J is coded with a change of the color from red to blue.

A. Effective tridiagonal Hamiltonian

The simplest way to apply our conjecture is to restrict the states involved in the dynamics, in zeroth order, to those that possess the set of the smallest (in absolute value) possible momenta for the given number of excitations in the chain. Now, we can build the zeroth-order Hamiltonian H_0 as a sparse matrix with non-vanishing elements – couplings and detunings, determined by the matrix elements between them. Explicit expressions for the latter can be found by means of (44). Concretely, H_0 connects only the states $|N; \vec{\eta}_0\rangle \leftrightarrow |N-1; \vec{\eta}_1\rangle \leftrightarrow |N-2; \vec{\eta}_2\rangle \leftrightarrow |N-3; \vec{\eta}_3\rangle \leftrightarrow |N-4; \vec{\eta}_4\rangle \leftrightarrow \dots$, where

$$\begin{aligned} \vec{\eta}_0 &= (\dots, 0, \dots), \\ \vec{\eta}_1 &= (\dots, 0, \frac{p}{2} + 1, 0, \dots), \\ \vec{\eta}_2 &= (\dots, 0, \frac{p}{2}, \frac{p}{2} + 1, 0, \dots), \\ \vec{\eta}_3 &= (\dots, 0, \frac{p}{2}, \frac{p}{2} + 1, \frac{p}{2} + 2, 0, \dots), \\ \vec{\eta}_4 &= (\dots, 0, \frac{p}{2} - 1, \frac{p}{2}, \frac{p}{2} + 1, \frac{p}{2} + 2, 0, \dots). \end{aligned} \quad (51)$$

Thence the full Hamiltonian matrix is written in the form

$$H = H_0 + V, \quad (52)$$

and we can proceed with the perturbation theory in the standard manner. It is seen, that in general the eigenvalues and eigenstates of H_0 , and so the correction terms has to be calculated numerically. Since we cannot find analytical formulas for the correction terms we will not be interested in them further.

The unperturbed Hamiltonian H_0 in (52), however, can be considered as an effective Hamiltonian approximating the actual problem, for a couple of periods and a small total number of excitations. After excluding the zero rows and columns the effective Hamiltonian is greatly reduced in size to a $(N+1) \times (N+1)$ matrix and takes a tridiagonal form. As we have already seen in Sec. VI for a single excitation, H_0 actually generates the exact dynamics. With an

increase of N the accuracy of this approximation decreases, because of the increasing number of possible routes from which the probability can leak out of the subspace spanned by the states $|N; \vec{\eta}_0\rangle, |N-1; \vec{\eta}_1\rangle, |N-2; \vec{\eta}_2\rangle, |N-3; \vec{\eta}_3\rangle, |N-4; \vec{\eta}_4\rangle, \dots$. In principle, with the increase of N , one can gradually add the most involved in the dynamics modes and still find relatively simple, more accurate, and small in size effective Hamiltonians.

For instance, in Fig. 5 we present both the results obtained with the use of the effective tridiagonal model and the exact solution. Comparison of the curves shows that for this specific choice of parameters, and for short-time dynamics, the deviation of the approximated from the exact reduced photon number is around 5%.

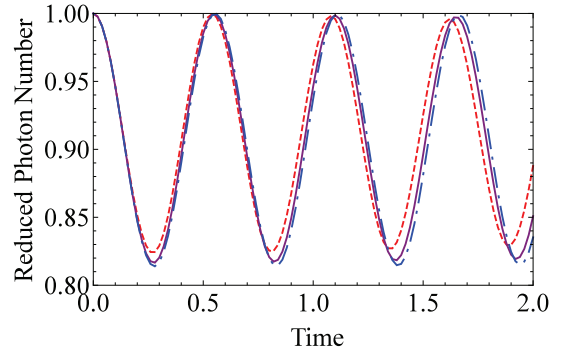


FIG. 5. (Color online) Dynamics of the reduced photon number – exact, represented with a solid purple curve; approximate, obtained with the use of the effective tridiagonal (subsec. VIII A) and Tavis-Cummings (subsec. VIII B) Hamiltonians and represented with dashed red and dashed-dotted blue curves, respectively. The parameters used for the computations are $N = 4, p = 12, J\tau/\hbar = 1, \Delta\tau = -12$. The dimensionless time t/τ is plotted on the abscissa.

B. Effective Tavis-Cummings model

Another possible choice for the effective Hamiltonian can be obtained under the assumption of large enough number of sites p when we can neglect the periodic boundary term \hat{H}_b (B4d) which is of order $O(p^{-1})$. This is equivalent to work only in the $\sigma = -1$ subspace. Further, since the states most involved in the dynamics are those with zero net momentum of the chain, we can find the zero-order Hamiltonian simply setting $k = 0$, which is $\Lambda_k = 1, \forall k$. Switching back to the spin- \hat{S} representation, we see that this is nothing but the Tavis-Cummings model, we have

$$\hat{H}_0 = \hbar\omega\hat{N} + (2J + \hbar\Delta)\hat{S}_z - \frac{\hbar\Omega}{\sqrt{2}} \left(\hat{a}_+ \hat{S}_+ + \hat{a}_+^\dagger \hat{S}_- \right). \quad (53)$$

Comments similar to the ones in the previous section can be made again. Namely, the correction terms will be given either by complex analytical formulas or computed numerically. For that reason we will not deal with the corrections, but rather will treat \hat{H}_0 as an effective approximation. The

effective Tavis-Cummings Hamiltonian approximates well (even better than the tridiagonal one) the actual problem for small values of N and for short times as seen in Fig. 5.

IX. PHOTON EMISSION

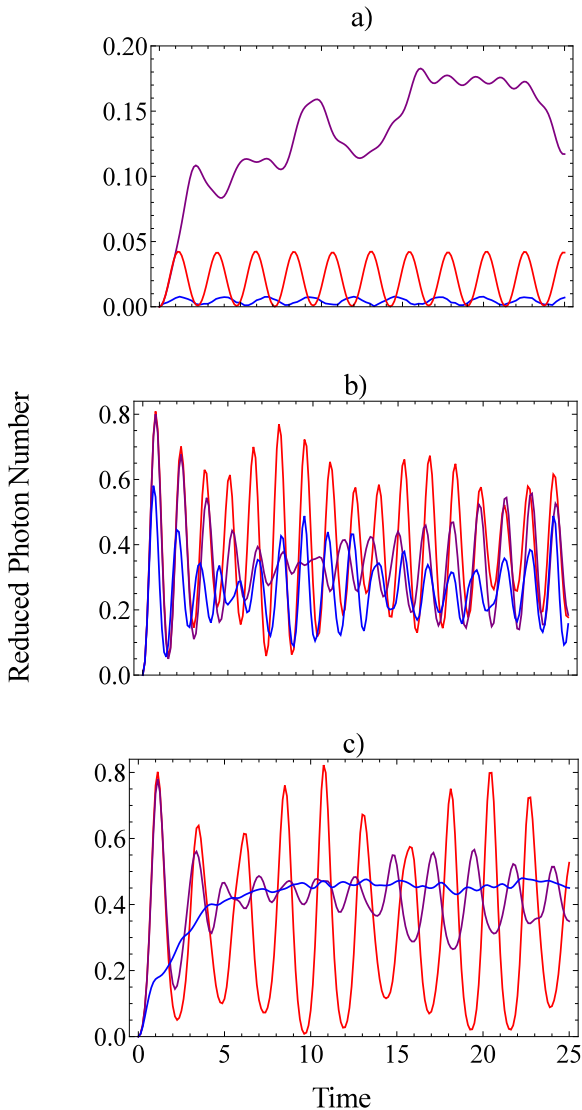


FIG. 6. (Color online) Long-term evolution of the reduced photon number $P_{\text{ph}}(t)$ for different couplings J is shown. In Figs. a) and b) the initial state is the ground state of the XY chain for anti-ferromagnetic and ferromagnetic case, respectively. The parameters used for the computations are $p = 12, N = 6, \Delta\tau = 0$, and $J\tau/\hbar = 0, 0.5, 3$ for Fig. a) and $J\tau/\hbar = 0, -0.5, -3$ for Fig. b). In Fig. c) the initial state is ferromagnetic with all spins (μ 's) up(down) $p = N = 12$, the coupling changes in the range $J\tau/\hbar = 0, -0.5, -3$ and $\Delta\tau = 0$. The dimensionless time t/τ is plotted on the abscissa. With the increase of absolute value of J the colors change from red to blue.

Now, let us consider some examples of the dynamics of

the system that begins its evolution from a state belonging to another class of initial conditions. The one in which any initial state contains all the excitations in the chain. We are interested in the on-resonance case ($\Delta = 0$) in order to obtain larger transfer of excitation from the chain to the field. Though that here we use initial conditions different than in the previous sections the long term behavior of the quantities is similar regardless of this choice – irregular oscillations around some average value.

The reduced photon number $P_{\text{ph}}(t)$ as a function of time and for different couplings J is shown in Fig. 6. Figures 6 a) and 6 b) represent the case when the initial state is the ground state of the XY model for anti-ferromagnetic ($J > 0$) and ferromagnetic ($J < 0$) cases, respectively, see Appendix B 2 b). In Fig. 6 c) the initial state is ferromagnetic with all spins up. Evidently, in small $|J|$ regime ($|J|\tau/\hbar \ll 1$) the dynamics is mainly determined by the one of the resonant Tavis-Cummings model. The behavior of most of the curves in the figures is oscillatory, and the frequency of these oscillations is barely dependent on J . We observe a reduction of the amplitude of oscillations with the increase of $|J|$, since viewed in the η -fermion basis, $|J|$ increases the effective detuning. In general, further increase of $|J|$ would cause the excitations to stay predominantly trapped in the chain, and thence, decrease of the averaged value of $P_{\text{ph}}(t)$. (The latter effect is not clearly seen in the figures but is additionally verified.) These observations are very well illustrated in Fig. 6 c) where, for the given class of initial conditions, the total number of excitations is maximally possible $N = p = 12$. In addition, the larger number of excitations in Fig. 6 c) in comparison with Figs. 6 a) and 6 b), leads to more modes involved in the dynamics and more intense exchange of excitations between the chain and the fields. As a result the oscillations of $P_{\text{ph}}(t)$ for large $|J|$ practically disappear. It stabilizes around some average value where an equilibrium between the absorbed and radiated photons from the chain is established. (See the curve corresponding to $J\tau/\hbar = -3$ in Fig. 6 c).)

Another thing to notice is the short-term dynamics in Fig. 6 c). Concretely, in the first period of oscillation the curves for $J\tau/\hbar = 0, -0.5$ lay very close to each other. Therefore, since for the Tavis-Cummings model ($J = 0$) the system pass through a superradiant behavior during the emission ($m(t) \approx 0, P_{\text{ph}}(t) \approx 1/2$), the same can be expected for small values of J [33]. In the second half-period the absorption in the "super" regime [34] is realized as well. The increase of J leads to the suppression of the oscillations involving superprocesses. In Figs. 6 a) and 6 b) the magnetization $m(t)$ coincides with $P_{\text{ph}}(t)$, and $m(t) \approx 0$ is realized periodically in Fig. 6 a) and only at the beginning in Fig. 6 b). In Fig. 6 a) the emission rate, as seen, is expected to be small. In the first period of oscillation, in Fig. 6 b), for $J\tau/\hbar = 0, -0.5$, however, we can make a guess that there is somewhat enhanced radiation. The above qualitative considerations are verified numerically by checking the condition

$$\left| \frac{I}{pI_0} \right| = \left| \frac{N(dP_{\text{ph}}(t)/dt)|_{\text{max}}}{pI_0} \right| > 1, \quad (54)$$

which signals abnormal radiation/absorption. Here I_0 and I are the maximum radiation rates of a single spin and of the studied system I , respectively. The condition (54) proves to be fulfilled very well (compatible with the expected values for superradiant behavior) for the first period for the case of $J\tau/\hbar = 0, -0.5$ in Fig. 6 c), and slightly for the first period for the case of $J\tau/\hbar = 0, -0.5$ in Fig. 6 b), as we have already discussed.

X. CONCLUSIONS

In conclusion, we considered the model of a periodic XY chain system, subject to a constant homogeneous magnetic field, and to a single-mode of quantized circularly polarized electromagnetic field. The geometry of the problem is chosen such that the constant component and the wave vector of the quantized component of the fields are perpendicular to the plane of the XY chain. The conditions for application of the rotating wave approximation to the Dicke part of the model are examined. We found that in addition to the conditions to discard the counter-rotating terms, in order to keep the rest of the Hamiltonian unaffected, the coupling between the spins has to be perturbatively small and all constituents (spins) of the XY chain has to interact with the field mode. Then, after application of successive Jordan-Wigner transformation and Fourier transform to the RWA Hamiltonian we continue the analysis in the basis, where the XY part of the Hamiltonian becomes diagonal. We introduced three quantities to describe the problem: reduced photon number, (dimensionless) magnetization per site and the ratio between the total number of excitations and the number of spins. The conservation of the total number of excitations relates them, so only two of these quantities can be considered as independent.

We were mostly interested in the case when the initial state is a product state of a number state of the field and the ground state of the XY model in the strong constant homogeneous field. We found the exact analytical solution of the problem in the single-excitation regime. We noticed that there are only two states involved in the dynamics – the state with the photon in the field, and the one with the excited zero-momentum mode of the chain. Then the problem effectively reduces to the solution of the well-known Jaynes-Cummings model, which reveals the quantum Rabi oscillations.

For the general case of more than one excitation we performed numerical computations. It is shown that for the studied choices of parameters (Δ always large), the reduced photon number and the magnetization per site also reveal a sort of oscillatory behavior with frequency dependent on the values of Δ and J for fixed Ω , and not so much on the values of p and N . Slight dependence of $P_{\text{ph}}(t)$ and strong dependence of $m(t)$ on N is established. Symmetry with respect to simultaneous changes $P_{\text{ph}}(t) \leftrightarrow m(t)$ and $p \leftrightarrow 2N$ is demonstrated. The increase of $|\Delta|$ is seen to lead to the reduction of the amplitude and increase of the frequency of the oscillations.

Based on the assumption that the vast part of the excitations are shared between the field and the zero-momentum modes of the chain we found two effective Hamiltonians. The first is an effective matrix tridiagonal Hamiltonian acting on the space spanned by the modes possessing zero net momentum, which have the smallest (in absolute value) set of momenta for a given number of excitations in the field. The second is the Tavis-Cummings effective Hamiltonian, found by smearing out the difference between even and odd subspaces and setting all the momenta to zero. The former (tridiagonal) Hamiltonian acts on the much reduced in size Hilbert subspace, that leads to a great simplification of the computations. The latter (Tavis-Cummings) Hamiltonian has the advantage that it is a well-known and largely studied model. It is demonstrated that the effective Hamiltonians generate short-time dynamics that provides a reasonable approximation for small number of total excitations.

The on-resonance situations, when the initial condition is such that the excitations reside in the XY chain, are also discussed. It is found that the long-term evolution brings the system, generally, in an oscillatory regime around some average value of the reduced photon number. The tendencies of the amplitude of the oscillations and of the average value of $P_{\text{ph}}(t)$ is to decrease with the increase of $|J|$, and for larger $|J|$ the amplitude of the oscillations decreases with the increase of N . A specific example is considered, with maximally excited XY chain part of the initial condition, and for small $|J|$, where the superradiant behavior is presented in the beginning of the emission.

The results presented here can be useful in studying problems as bosonic mode in a spin-bath, spin chains or linear molecular aggregates in a single-mode cavity, and superradiating/superabsorbing systems.

ACKNOWLEDGMENTS

The authors would like to thank A. A. Donkov for useful discussions during an early stage of this project. S. Varbe is supported by the Bulgarian Ministry of Education and Science under the National Research Programme “Young scientists and postdoctoral researchers” approved by DCM under No 577/17.08.2018. I. Boradjiev, H. Tonchev and H. Chamati would like to acknowledge the financial support by Grant DN0818/14.12.2016 of the Bulgarian Science Foundation.

Appendix A: Rotating wave approximation

In this Appendix we present the derivation of the Hamiltonian (15a) following the approach presented in [35]. To this end, we make use of the formula

$$\overline{T} \exp \left\{ \int_{t_0}^t d\tau [\hat{A} + \hat{B}(\tau)] \right\} = \exp [\hat{A}(t - t_0)] \overline{T} \exp \left[\int_{t_0}^t d\tau \hat{B}(\tau) \right], \quad (\text{A1a})$$

where

$$\hat{B}(t) = \exp[-\hat{A}(t-t_0)] \hat{B} \exp[\hat{A}(t-t_0)], \quad (\text{A1b})$$

and \overleftarrow{T} stands for the time-ordering of the exponent.

The formal solution of the Schrödinger equation

$$i\hbar \frac{d}{dt} |\psi\rangle = \hat{H} |\psi\rangle, \quad |\psi_0\rangle = |\psi(0)\rangle, \quad (\text{A2})$$

reads

$$|\psi\rangle = \overleftarrow{T} \exp\left(-\frac{i}{\hbar} \int_0^t d\tau \hat{H}\right) |\psi_0\rangle. \quad (\text{A3})$$

Identifying in (11) the operators \hat{A} with $-i\omega(\hat{n}_+ + \hat{n}_- + \frac{p}{2} + \sum_{i=1}^p \hat{S}_{iz})$ and \hat{B} with $-\frac{i}{\hbar}(\hat{H}^{XY} + \hat{H}^D)$, respectively, we get

$$\begin{aligned} |\psi\rangle = & \exp\left(-i\omega\left(\hat{n}_+ + \hat{n}_- + \frac{p}{2} + \sum_{i=1}^p \hat{S}_{iz}\right)T\right) \\ & \times \overleftarrow{T} \exp\left(-\frac{i}{\hbar} \int_0^T dt \hat{H}^{XY+D}\right) |\psi_0\rangle, \end{aligned} \quad (\text{A4})$$

where

$$\begin{aligned} \hat{H}^{XY+D} = & \hat{H}_{>p}^{XY} + \hat{H}_{<p}^{XY} + \hbar\omega_1 \sum_{i>p} \hat{S}_{iz} + \hat{H}^{RWA} \\ & + J \sum_{i>p>j} (\hat{S}_{i+} \hat{S}_{j-} e^{-i\omega t} + \hat{S}_{i-} \hat{S}_{j+} e^{+i\omega t}) \\ & - \frac{\hbar\Omega}{\sqrt{2}} \sum_{i=1}^p (\hat{a}_-^\dagger \hat{S}_{i+} e^{2i\omega t} + \hat{a}_- \hat{S}_{i-} e^{-2i\omega t}), \end{aligned} \quad (\text{A5a})$$

with

$$\hat{H}_{>p}^{XY} = J \sum_{i>j>p} (\hat{S}_{i+} \hat{S}_{j-} + \hat{S}_{i-} \hat{S}_{j+}), \quad (\text{A5b})$$

$$\hat{H}_{<p}^{XY} = J \sum_{p>i>j} (\hat{S}_{i+} \hat{S}_{j-} + \hat{S}_{i-} \hat{S}_{j+}), \quad (\text{A5c})$$

and

$$\hat{H}^{RWA} = \hbar\Delta \sum_{i=1}^p \hat{S}_{iz} - \frac{\hbar\Omega}{\sqrt{2}} \sum_{i=1}^p (\hat{a}_+ \hat{S}_{i+} + \hat{a}_+^\dagger \hat{S}_{i-}). \quad (\text{A5d})$$

Now we apply formula (A1) for the time-ordered exponent in (A4), with the identification $\hat{A} = -(i/\hbar)\hat{H}^{RWA}$ and $\hat{B} = -(i/\hbar)(\hat{H}^{XY+D} - \hat{H}^{RWA})$.

$$\begin{aligned} & \overleftarrow{T} \exp\left(-\frac{i}{\hbar} \int_0^T dt \hat{H}^{XY+I}\right) \\ & = \exp\left(-\frac{i}{\hbar} \hat{H}^{RWA} T\right) \overleftarrow{T} \exp\left(-\frac{i}{\hbar} \int_0^T dt \hat{H}^{XY+D-RWA}\right), \end{aligned} \quad (\text{A6a})$$

with

$$\begin{aligned} \hat{H}^{XY+D-RWA} = & \hat{H}_{>p}^{XY} + \hat{H}_{<p}^{XY} + \hbar\omega_1 \sum_{i>p} \hat{S}_{iz} \\ & + J \sum_{i>p>j} [\hat{S}_{i+} \hat{S}_{j-}(t) e^{-i\omega t} + \hat{S}_{i-} \hat{S}_{j+}(t) e^{+i\omega t}] \\ & - \frac{\hbar\alpha - \Omega}{\sqrt{2}} \sum_{i=1}^p [\hat{S}_{i+}(t) e^{2i\omega t} + \hat{S}_{i-}(t) e^{-2i\omega t}], \end{aligned} \quad (\text{A6b})$$

and

$$\hat{H}_{<p}^{XY} = J \sum_{p>i>j} [\hat{S}_{i+}(t) \hat{S}_{j-}(t) + \hat{S}_{i-}(t) \hat{S}_{j+}(t)]. \quad (\text{A6c})$$

To derive the above we proceed as follows: We introduce a new set of half-spin operators

$$\begin{aligned} \hat{S}_{i+} = & \frac{2\Gamma}{\Lambda} \hat{R}_{iz} + \frac{i}{2} \left(1 + \frac{\delta}{\Lambda}\right) \hat{R}_{i+} + \frac{i}{2} \left(1 - \frac{\delta}{\Lambda}\right) \hat{R}_{i-}, \\ \hat{S}_{i-} = & \frac{2\Gamma}{\Lambda} \hat{R}_{iz} - \frac{i}{2} \left(1 - \frac{\delta}{\Lambda}\right) \hat{R}_{i+} - \frac{i}{2} \left(1 + \frac{\delta}{\Lambda}\right) \hat{R}_{i-}, \\ \hat{S}_{iz} = & \frac{\delta}{\Lambda} \hat{R}_{iz} - \frac{i\Gamma}{\Lambda} (\hat{R}_{i+} - \hat{R}_{i-}), \quad i = 1, \dots, p, \end{aligned} \quad (\text{A7})$$

where

$$[\hat{R}_{i+}, \hat{R}_{i-}] = 2\hat{R}_{iz}, \quad [\hat{R}_{iz}, \hat{R}_{i\pm}] = \pm\hat{R}_{i\pm}. \quad (\text{A8})$$

We consider the case of a large photon number, so we make the replacements

$$\hat{a}_\pm, \hat{a}_\pm^\dagger \rightarrow \alpha_\pm. \quad (\text{A9})$$

Further, we define the remaining free constants that parameterize the transformation

$$\delta = \Delta, \quad \sqrt{2}\Gamma = -\alpha_+ \Omega, \quad \Lambda = \sqrt{4\Gamma^2 + \delta^2}. \quad (\text{A10})$$

In this representation we have

$$\hat{H}^{RWA} = \hbar\Lambda \sum_{i=1}^p \hat{R}_{iz}. \quad (\text{A11})$$

The operators $\hat{S}_{i\pm}(t)$ defined via

$$\hat{S}_{i\pm}(t) = \exp\left(i \frac{\hat{H}^{RWA}}{\hbar} t\right) \hat{S}_{i\pm} \exp\left(-i \frac{\hat{H}^{RWA}}{\hbar} t\right), \quad (\text{A12})$$

are easy to calculate explicitly with the use of the formulas

$$\exp(i\Lambda t \hat{R}_{iz}) \hat{R}_{i\pm} \exp(-i\Lambda t \hat{R}_{iz}) = \exp(\pm i\Lambda t) \hat{R}_{i\pm}. \quad (\text{A13})$$

Next, we apply formula (A1) for the time-ordered exponent in the right-hand side of (A6a), with the identification $\hat{A} = -(i\omega_1 \sum_{i>p} \hat{S}_{iz})$ and $\hat{B} = -(i/\hbar)(\hat{H}^{XY+D-RWA} - \hbar\omega_1 \sum_{i>p} \hat{S}_{iz})$,

$$\begin{aligned} & \overleftarrow{T} \exp\left(-\frac{i}{\hbar} \int_0^T dt \hat{H}^{XY+D-RWA}\right) \\ & = \exp\left(-i\omega_1 \sum_{i>p} \hat{S}_{iz} T\right) \overleftarrow{T} \exp\left(-\frac{i}{\hbar} \int_0^T dt \hat{H}^{XY+D-RWA-Z}\right), \end{aligned} \quad (\text{A14})$$

with

$$\begin{aligned} \hat{H}^{XY+D-RWA-Z} = & \hat{H}_{>p}^{XY} + \hat{H}_{<p}^{XY} \\ & + J \sum_{i>p>j} [\hat{S}_{i+} \hat{S}_{j-}(t) e^{+i\Delta t} + \hat{S}_{i-} \hat{S}_{j+}(t) e^{-i\Delta t}] \\ & - \frac{\hbar\alpha - \Omega}{\sqrt{2}} \sum_{i=1}^p [\hat{S}_{i+}(t) e^{2i\omega t} + \hat{S}_{i-}(t) e^{-2i\omega t}]. \end{aligned} \quad (\text{A15})$$

The application of the formula (A1) for the time-ordered exponent in the right-hand side of (A14), with the identification $\hat{A} = -(i/\hbar)\hat{H}_{>p}^{XY}$ and $\hat{B} = -(i/\hbar)(\hat{H}^{XY+D-RWA-Z} - \hat{H}_{>p}^{XY})$, gives

$$\overline{T} \exp\left(-\frac{i}{\hbar} \int_0^T dt \hat{H}^{XY+D-RWA-Z}\right) = \exp\left(-\frac{i}{\hbar} \hat{H}_{>p}^{XY} T\right) \overline{T} \exp\left(-\frac{i}{\hbar} \int_0^T dt \hat{H}^{XY+D-RWA-Z-(XY>p)}\right), \quad (\text{A16a})$$

with

$$\begin{aligned} \hat{H}^{XY+D-RWA-Z-(XY>p)} &= \hat{H}_{<p}^{XY} + J \sum_{i>p \geq j} [\hat{S}'_{i+}(t) \hat{S}_{j-}(t) e^{+i\Delta t} + \hat{S}'_{i-}(t) \hat{S}_{j+}(t) e^{-i\Delta t}] \\ &\quad - \frac{\hbar\alpha - \Omega}{\sqrt{2}} \sum_{i=1}^p [\hat{S}'_{i+}(t) e^{2i\omega t} + \hat{S}'_{i-}(t) e^{-2i\omega t}], \end{aligned} \quad (\text{A16b})$$

where

$$\begin{aligned} \hat{S}'_{i\pm}(t) &= \exp\left(+\frac{i}{\hbar} \hat{H}_{>p}^{XY} t\right) \hat{S}_{i\pm} \exp\left(-\frac{i}{\hbar} \hat{H}_{>p}^{XY} t\right) \\ &= \hat{S}_{i\pm} + \left[\frac{i}{\hbar} \hat{H}_{>p}^{XY} t, \hat{S}_{i\pm}\right] + \dots \end{aligned} \quad (\text{A16c})$$

From now on we work with one-dimensional chain in

nearest-neighbor approximation. In this case the sum involving $\hat{S}'_{i\pm}(t)$ is reduced to a single term ($i = p + 1$). Imposing the condition $JT/\hbar \ll 1$, we have $\hat{S}'_{i\pm}(t) = \hat{S}_{i\pm} + O(tJ/\hbar)$, $t \in [0, T]$.

Again, the application of the formula (A1) for the time-ordered exponent in the right-hand side of (A16a), with the identification $\hat{A} = -(i/\hbar) \hat{H}_{<p}^{XY}$ and $\hat{B} = -(i/\hbar) (\hat{H}^{XY+D-RWA-Z-(XY>p)} - \hat{H}_{<p}^{XY})$, gives

$$\overline{T} \exp\left(-\frac{i}{\hbar} \int_0^T dt \hat{H}^{XY+D-RWA-Z-(XY>p)}\right) = \exp\left(-\frac{i}{\hbar} \hat{H}_{<p}^{XY} T\right) \overline{T} \exp\left(-\frac{i}{\hbar} \int_0^T dt \hat{H}^{XY+D-RWA-Z-(XY>p)-(XY<p)}\right), \quad (\text{A17a})$$

with

$$\begin{aligned} \hat{H}^{XY+D-RWA-Z-(XY>p)-(XY<p)} &= \\ J \sum_{i>p \geq j} &[\hat{S}''_{i+}(t) \hat{S}''_{j-}(t) e^{+i\Delta t} + \hat{S}''_{i-}(t) \hat{S}''_{j+}(t) e^{-i\Delta t}] \\ - \frac{\hbar\alpha - \Omega}{\sqrt{2}} &\sum_{i=1}^p [\hat{S}''_{i+}(t) e^{2i\omega t} + \hat{S}''_{i-}(t) e^{-2i\omega t}] \\ + \hat{H}_{<p}^{XY} - \hat{H}_{<p}^{XY}, & \end{aligned} \quad (\text{A17b})$$

$$\begin{aligned} \hat{S}''_{i\pm}(t) &= \exp\left(+\frac{i}{\hbar} \hat{H}_{<p}^{XY} t\right) \hat{S}_{i\pm}(t) \exp\left(-\frac{i}{\hbar} \hat{H}_{<p}^{XY} t\right) \\ &= \hat{S}_{i\pm}(t) + \left[\frac{i}{\hbar} \hat{H}_{<p}^{XY} t, \hat{S}_{i\pm}(t)\right] + \dots \end{aligned} \quad (\text{A17c})$$

Once more we use the requirement $JT/\hbar \ll 1$ to ensure the expansion $\hat{S}''_{i\pm}(t) = \hat{S}_{i\pm}(t) + O(tJ/\hbar)$.

Strictly speaking, for the validity of RWA, the frequency ω must be orders of magnitude larger than any other quantity. In addition, we specifically assume the fulfillment of the condition $\frac{\alpha + \Omega}{\omega} \ll 1$. To employ the modified for the case RWA is equivalent to approximate the T -exponent in

$$\begin{aligned} \overline{T} \exp\left(-\frac{i}{\hbar} \int_0^T dt \hat{H}^{XY+D-RWA-Z-(XY>p)-(XY<p)}\right) &\approx \overline{T} \exp\left\{-\frac{i}{\hbar} \int_0^T dt \left[\left(-\frac{\hbar\alpha - \Omega}{\sqrt{2}}\right) \sum_{i=1}^p (\hat{S}_{i+}(t) e^{2i\omega t} + \hat{S}_{i-}(t) e^{-2i\omega t}) \right. \right. \\ &\quad + J \sum_{i>p \geq j} (\hat{S}_{i+} \hat{S}_{j-}(t) e^{+i\Delta t} + \hat{S}_{i-} \hat{S}_{j+}(t) e^{-i\Delta t}) \\ &\quad \left. \left. + J \sum_{p>i \geq j} (\hat{S}_{i+}(t) \hat{S}_{j-}(t) + \hat{S}_{i-}(t) \hat{S}_{j+}(t)) - J \sum_{p>i \geq j} (\hat{S}_{i+} \hat{S}_{j-} + \hat{S}_{i-} \hat{S}_{j+}) \right] \right\}. \end{aligned} \quad (\text{A18})$$

with the unity operator. To this end, it is sufficient to analyze the following expressions entering (A18) as summands.

(i) Expressions for the Dicke part (first term in the rhs of

(A18)):

$$1) \quad I_1 = \int_0^T dt \cos(2\omega t) = \frac{\sin(2\omega T)}{2\omega}, \quad (\text{A19})$$

$$\left| i\sqrt{2}p \frac{\alpha - \Omega \Gamma}{\Lambda} I_1 \right| \lesssim \begin{cases} p \left| \frac{\alpha - \Omega}{2\omega} \right|, & \text{for } \Delta \rightarrow 0, \\ p \left| \frac{\alpha - \Omega}{2\omega} \right| \left| \frac{\alpha + \Omega}{\omega} \right|, & \text{for } \Delta \rightarrow -\omega. \end{cases} \quad (\text{A20})$$

$$2) \quad (I_2^-)^* = I_2^+ = \int_0^T dt e^{i\Lambda t} \left(i \frac{\delta}{\Lambda} \cos(2\omega t) - \sin(2\omega t) \right) = \frac{2\omega - \delta + e^{i\Lambda T} \left[i \sin(2\omega T) \left(\Lambda - 2\omega \frac{\delta}{\Lambda} \right) - \cos(2\omega T) (2\omega - \delta) \right]}{\Lambda^2 - 4\omega^2}, \quad (\text{A21})$$

$$\left| i p \frac{\alpha - \Omega}{\sqrt{2}} I_2^\pm \right| \lesssim \begin{cases} p \left| \frac{\alpha - \Omega}{\omega} \right|, & \text{for } \Delta \rightarrow 0, \\ 3p \left| \frac{\alpha - \Omega}{\omega} \right|, & \text{for } \Delta \rightarrow -\omega. \end{cases} \quad (\text{A22})$$

(ii) Expressions for the field-boundary XY term [36], (second term in the rhs of (A18)):

$$3) \quad (I_3^-)^* = I_3^+ = \int_0^T dt e^{i\Delta t} = -i \frac{e^{i\Delta T} - 1}{\Delta}, \quad (\text{A23})$$

$$\left| -i \frac{JT}{\hbar \Lambda} I_3^\pm \right| \lesssim \begin{cases} \left| \frac{J}{\hbar \Delta} \right|, & \text{for } \Delta \rightarrow 0 \text{ [37]}, \\ \left| \frac{2J}{\hbar \omega} \right| \left| \frac{\alpha + \Omega}{\omega} \right|, & \text{for } \Delta \rightarrow -\omega. \end{cases} \quad (\text{A24})$$

$$4) \quad (I_{4a}^-)^* = I_{4a}^+ = -i \int_0^T dt e^{i(\Lambda + \Delta)t} = -\frac{e^{i(\Lambda + \Delta)T} - 1}{\Lambda + \Delta}, \quad (\text{A25})$$

$$(I_{4b}^-)^* = I_{4b}^+ = i \int_0^T dt e^{i(\Lambda - \Delta)t} = \frac{e^{i(\Lambda - \Delta)T} - 1}{\Lambda - \Delta}, \quad (\text{A26})$$

$$\left| -i \frac{J}{2\hbar} \left(1 - \frac{\delta}{\Lambda} \right) I_{4a}^\pm \right| \lesssim \begin{cases} \left| \frac{J}{\hbar \alpha + \Omega} \right|, & \text{for } \Delta \rightarrow 0, \\ \left| 2 \frac{J}{\hbar \omega} \left(\frac{\omega}{\alpha + \Omega} \right)^2 \right|, & \text{for } \Delta \rightarrow -\omega \text{ [38]}, \end{cases} \quad (\text{A27})$$

$$\left| -i \frac{J}{2\hbar} \left(1 + \frac{\delta}{\Lambda} \right) I_{4b}^\pm \right| \lesssim \begin{cases} \left| \frac{J}{\hbar \alpha + \Omega} \right|, & \text{for } \Delta \rightarrow 0, \\ \left| \frac{1}{2} \frac{J}{\hbar \omega} \left(\frac{\alpha + \Omega}{\omega} \right)^2 \right|, & \text{for } \Delta \rightarrow -\omega. \end{cases} \quad (\text{A28})$$

(iii) Expressions for the XY part interacting with the field mode (last two terms in the rhs of (A18)):

$$5) \quad (I_5^-)^* = I_5^+ = i \int_0^T dt (e^{i\Lambda t} - 1) = \frac{e^{i\Lambda T} - 1}{\Lambda} - iT, \quad (\text{A29})$$

$$\left| -i p \frac{JT\delta}{\hbar \Lambda^2} I_5^\pm \right| \lesssim \begin{cases} p \left| \frac{JT}{2\hbar \alpha + \Omega} \right| \left| \frac{2}{\alpha + \Omega T} + 1 \right| \rightarrow 0, & \text{for } \Delta \rightarrow 0, \\ 2p \left| \frac{J}{\hbar \omega} \right| \left| \frac{\alpha + \Omega}{\omega} \right|, & \text{for } \Delta \rightarrow -\omega. \end{cases} \quad (\text{A30})$$

$$6) \quad (I_6^-)^* = I_6^+ = \int_0^T dt (e^{2i\Lambda t} - 1) = -i \frac{e^{2i\Lambda T} - 1}{2\Lambda} - T, \quad (\text{A31})$$

$$\left| -i p \frac{J}{2\hbar} \left(1 - \frac{\delta^2}{\Lambda^2} \right) I_6^\pm \right| \lesssim \begin{cases} p \left| \frac{JT}{2\hbar} \right| \left| \frac{1}{\alpha + \Omega T} + 1 \right|, & \text{for } \Delta \rightarrow 0 \text{ [39]}, \\ p \left| \frac{J}{\hbar \omega} \right| \left(\frac{\alpha + \Omega}{\omega} \right)^2, & \text{for } \Delta \rightarrow -\omega. \end{cases} \quad (\text{A32})$$

From all of the above estimates we can conclude that:

(i) Executing RWA for the Dicke part is possible given that

$$\frac{\alpha + \Omega}{\omega} \ll 1, \quad p \frac{\alpha - \Omega}{\omega} \ll 1, \quad \frac{JT}{\hbar} \ll 1. \quad (\text{A33})$$

(ii) In general, RWA will alter the field-boundary XY term and it will be non-negligible. (We have to recall, however, that the boundary term is of order $O(p^{-1})$, and so, for a very specific choice of parameters it may be considered small.)

(iii) To keep the interacting with the field mode XY terms unchanged under RWA we need to fulfill the following conditions. In the near-resonant case ($\Delta \rightarrow 0$), we require that

$$p \frac{JT}{\hbar} \ll 1, \quad (\text{A34})$$

and in the large detuning case ($\Delta \rightarrow -\omega$), we require

$$p \frac{J}{\hbar \omega} \lesssim 1. \quad (\text{A35})$$

Performing RWA without affecting the XY parts of the Hamiltonian needs the elimination of the field-boundary XY term. This can be achieved simply by considering a XY chain coupled to a photon mode with all of its spins.

Appendix B: Diagonalization of XY part of the Hamiltonian. Ground state of the XY model in a strong constant homogeneous field.

In this Appendix we briefly describe the transformations that diagonalize the XY part of Hamiltonian (15) and find its ground states and corresponding energies.

1. Diagonalization of XY part of the Hamiltonian

We consider the periodic XY model consisting of even number of spins in the nearest-neighbor approximation.

Note that in the case of periodic boundary conditions,

$$\hat{S}_{p+1\pm} = \hat{S}_{1\pm}, \quad (\text{B1})$$

we have to add to the XY part of the Hamiltonian (15a) the term

$$J(\hat{S}_{1+}\hat{S}_{p-} + \hat{S}_{1-}\hat{S}_{p+}). \quad (\text{B2})$$

To begin with, we employ the Jordan-Wigner transformation, i.e. we introduce a set of spinless Fermi operators

$$\hat{S}_{i-} = \exp\left(-i\pi \sum_{j=1}^{i-1} \hat{c}_j^\dagger \hat{c}_j\right) \hat{c}_i, \\ \hat{S}_{i+} = \hat{c}_i^\dagger \exp\left(i\pi \sum_{j=1}^{i-1} \hat{c}_j^\dagger \hat{c}_j\right),$$

obeying the canonical anti-commutation relations

$$\{\hat{c}_i, \hat{c}_j^\dagger\} = \delta_{ij}, \quad \{\hat{c}_i, \hat{c}_j\} = \{\hat{c}_i^\dagger, \hat{c}_j^\dagger\} = 0. \quad (\text{B3})$$

In terms of \hat{c} and \hat{c}^\dagger the expression for the Hamiltonian (15a) becomes [40]

$$\hat{H} = \hat{H}_p + \hat{H}_i + \hat{H}_b, \quad (\text{B4a})$$

with

$$\hat{H}_p = J \sum_{i=1}^p \left(\hat{c}_{i+1}^\dagger \hat{c}_i + \hat{c}_i^\dagger \hat{c}_{i+1} \right) + \hbar \Delta \sum_{i=1}^p \left(\hat{c}_i^\dagger \hat{c}_i - \frac{1}{2} \right), \quad (\text{B4b})$$

$$\hat{H}_i = -\frac{\hbar \Omega}{\sqrt{2}} \sum_{i=1}^p \left[\hat{a}_+ \hat{c}_i^\dagger \exp \left(i\pi \sum_{j=1}^{i-1} \hat{c}_j^\dagger \hat{c}_j \right) + h.c. \right], \quad (\text{B4c})$$

$$\hat{H}_b = -J \left(\hat{c}_1^\dagger \hat{c}_p + \hat{c}_p^\dagger \hat{c}_1 \right) (P+1), \quad (\text{B4d})$$

where in the first term in the definition of the periodic part \hat{H}_p it is understood that $\hat{c}_{p+1} \rightarrow \hat{c}_1$ and P is the fermion parity operator

$$P = \exp(i\pi \mathcal{N}), \quad \mathcal{N} = \sum_{j=1}^p \hat{c}_j^\dagger \hat{c}_j. \quad (\text{B5})$$

Observe that P is a constant of motion with respect to \hat{H}_p as

$$[P, \hat{H}_p] = 0, \quad (\text{B6})$$

and accepts two values $-P = +1$ for even and $P = -1$ for odd number of fermions, respectively. Therefore, the periodic XY part \hat{H}_p can be separately diagonalized in two subspaces with different parities, labeled by σ , see for example [23, 25, 29]. The identification is as follows: $\sigma = +1$ corresponds to a c -fermion system with imposed anti-periodic boundary conditions ($\hat{H}_b \neq 0$) and even number of excitations, while $\sigma = -1$ corresponds to the one with periodic boundary conditions ($\hat{H}_b = 0$) and with odd number of excitations.

Further, we rewrite the off-diagonal part of $\hat{H}_p + \hat{H}_b$, as

$$2J \sum_{i,j=1}^p \hat{c}_i^\dagger A_{ij}^\sigma \hat{c}_j, \quad (\text{B7a})$$

where

$$A_{ij}^\sigma = \frac{1}{2} [\delta_{ij+1} + \delta_{ji+1} - (P+1)(\delta_{i1}\delta_{jp} + \delta_{ip}\delta_{j1})],$$

$$\delta_{pp+1} = \delta_{p1}, \quad \delta_{p+1p} = \delta_{1p}. \quad (\text{B7b})$$

It is clear that A^σ are real and symmetric matrices. Hence, their eigenvalues Λ_k are real

$$\Lambda_{k\sigma} = \cos(k^\sigma), \quad (\text{B8})$$

$$k_\eta^\sigma = -\pi + \left(2\eta + \frac{\sigma-3}{2} \right) \frac{\pi}{p}, \quad \eta = 1, 2, \dots, p, \quad (\text{B9})$$

and their eigenvectors $\phi_k^{(\sigma)}$ are orthogonal, and can be normalized to give

$$\phi_{kj}^{(\sigma)} = \frac{1}{\sqrt{p}} e^{ik^\sigma j}, \quad \sum_{i=1}^p \phi_{ki}^{(\sigma)} \phi_{k'i}^{(\sigma)*} = \delta_{kk'}. \quad (\text{B10})$$

The Fourier expansions of \hat{c} and \hat{c}^\dagger , by means of which A^σ can be diagonalized, are defined via

$$\hat{c}_i = \sum_{k \in BZ} \phi_{ki}^{(\sigma)} \hat{\eta}_{k\sigma}, \quad \hat{c}_i^\dagger = \sum_{k \in BZ} \phi_{ki}^{(\sigma)*} \hat{\eta}_{k\sigma}^\dagger. \quad (\text{B11})$$

As can be easily checked the Fourier transforms $\hat{\eta}_{k\sigma}$ and $\hat{\eta}_{k\sigma}^\dagger$ are also Fermion operators

$$\{\hat{\eta}_{k\sigma}, \hat{\eta}_{k'\sigma}^\dagger\} = \delta_{kk'}, \quad \{\hat{\eta}_{k\sigma}, \hat{\eta}_{k'\sigma}\} = \{\hat{\eta}_{k\sigma}^\dagger, \hat{\eta}_{k'\sigma}^\dagger\} = 0. \quad (\text{B12})$$

Eventually, substituting the expansions (B11) for \hat{c} and \hat{c}^\dagger into the expression for \hat{H} (B4a) we end up with Hamiltonian (16).

2. Ground state of the XY model

For our further goals, we also need some of the zero-temperature properties of the XY spin model. We consider the ground states and energies for the cases of XY model with and without the external field B_z .

a. Ground state of the XY model in a strong constant homogeneous field

For the XY model in the external field B_z , we have

$$\begin{aligned} \hat{H}^{XY+B} &= \hbar \omega_1 \sum_i \hat{S}_{iz} + 2J \sum_i (\hat{S}_{ix} \hat{S}_{i+1x} + \hat{S}_{iy} \hat{S}_{i+1y}) \\ &= \sum_{\sigma=\pm} \frac{1+\sigma P}{2} \sum_{k \in BZ} \varepsilon_\sigma(k) \left(\hat{\eta}_{k\sigma}^\dagger \hat{\eta}_{k\sigma} - \frac{1}{2} \right) \frac{1+\sigma P}{2}, \end{aligned} \quad (\text{B13})$$

$$\varepsilon_\sigma(k) = 2J \Lambda_{k\sigma} + \hbar \omega_1, \quad (\text{B14})$$

which is a particular case of (16a) when no oscillating field in the $x-y$ plane is present ($\Omega = 0, \Delta \rightarrow \omega_1$). Assuming anti-ferromagnetic XY chain ($J > 0$), one distinguishes three cases $-\hbar \omega_1 < 2J, \hbar \omega_1 \leq -2J$, and $\hbar \omega_1 \geq 2J$. Henceforth we will consider the regime when $\hbar \omega_1 \geq 2J$.

The values of the Fermi momentum k_F for the free fermion system in (B13) are determined by the condition

$$\varepsilon_\sigma(k_F) = 2J \Lambda_{k\sigma} + \hbar \omega_1 = 0, \quad (\text{B15})$$

from where we find that the Fermi surface consists of the two symmetric points

$$k_{\sigma F} = \pm \pi \quad (\text{B16})$$

located at the edges of the BZ . Here $\hbar \omega_1$ plays the role of chemical potential. Since in the regime considered the energy $\varepsilon(k_F)$ is nonnegative and determines the minimum of the dispersion relation, i.e.

$$\varepsilon(k) \geq \varepsilon(k_F) \geq 0, \quad (\text{B17})$$

the ground state $|0\rangle$ is characterized by lack of η -quasi-particles

$$|0\rangle = |0, 0, \dots, 0\rangle, \quad (\text{B18})$$

and hence, ferromagnetic order

$$M = \mu p, \quad (\text{B19})$$

where μ is the projection of the magnetic moment in a single site on the z -axis and M is the magnetic moment of the chain. (Recall, that we have assumed $\hat{\mu}_S = -2\mu\hat{S}$.)

b. Ground state of the XY model

The values of the Fermi momentum k_F in the case of no field presented are determined by the condition

$$\varepsilon_\sigma(k_F) = 2J\Lambda_{k\sigma} = 0. \quad (\text{B20})$$

Now, the Fermi surface consists of the two symmetric points

$$k_{\sigma F} = \pm \frac{\pi}{2}. \quad (\text{B21})$$

The filling numbers of the states for anti-ferromagnetic case ($J > 0$) is

$$n_{k\sigma} = 1 \text{ for } [-\pi, -k_{\sigma F}] \cup [k_{\sigma F}, \pi], \quad (\text{B22})$$

$$n_{k\sigma} = 0 \text{ for } [-k_{\sigma F}, k_{\sigma F}]. \quad (\text{B23})$$

For the ground energy and ground state, we obtain

$$E_\sigma(k_F) = 2J \sum_{k \in BZ} \Lambda_k \hat{\eta}_k^\dagger \hat{\eta}_k, \quad (\text{B24})$$

$$|g\rangle = |1, 1, \dots, 1, 0, 0, \dots, 0, 1, 1, \dots, 1\rangle, \quad (\text{B25})$$

respectively. The system is characterized by anti-ferromagnetic order, so its magnetic moment vanishes,

$$M = -\mu \left(\sum_{k \in [-\pi, -k_{\sigma F}]} 1 + \sum_{k \in [k_{\sigma F}, \pi]} 1 - \sum_{k \in [-k_{\sigma F}, k_{\sigma F}]} 1 \right) = 0. \quad (\text{B26})$$

In the ferromagnetic case ($J < 0$) we have

$$E_\sigma(k_F) = 2J \sum_{k \in BZ} \Lambda_k \hat{\eta}_k^\dagger \hat{\eta}_k = -2|J| \sum_{k \in BZ} \Lambda_k \hat{\eta}_k^\dagger \hat{\eta}_k, \quad (\text{B27})$$

$$|g'\rangle = |0, 0, \dots, 0, 1, \dots, 1, 0, 0, \dots, 0\rangle, \quad (\text{B28})$$

and

$$M = \mu p = 0. \quad (\text{B29})$$

-
- [1] A. Kirilyuk, A. V. Kimel, and T. Rasing, Ultrafast optical manipulation of magnetic order, *Rev. Mod. Phys.* **82**, 2731 (2010).
- [2] C. Noh and D. G. Angelakis, Quantum simulations and many-body physics with light, *Rep. Prog. Phys.* **80**, 016401 (2017).
- [3] M. Harder and C.-M. Hu, Cavity Spintronics: An Early Review of Recent Progress in the Study of Magnon-Photon Level Repulsion, in *Solid State Physics*, Vol. 69 (Elsevier, 2018) pp. 47–121.
- [4] J.-Y. Bigot and M. Vomir, Ultrafast magnetization dynamics of nanostructures: Ultrafast magnetization dynamics of nanostructures, *Annalen der Physik* **525**, 2 (2013).
- [5] A. Kimel, A. Kirilyuk, and T. Rasing, Femtosecond optomagnetics: ultrafast laser manipulation of magnetic materials, *Laser & Photonics Review* **1**, 275 (2007).
- [6] Ö. O. Soykal and M. E. Flatté, Strong Field Interactions between a Nanomagnet and a Photonic Cavity, *Phys. Rev. Lett.* **104**, 077202 (2010).
- [7] D. Bossini, A. M. Kalashnikova, R. V. Pisarev, T. Rasing, and A. V. Kimel, Controlling coherent and incoherent spin dynamics by steering the photoinduced energy flow, *Phys. Rev. B* **89**, 060405 (2014).
- [8] F. Hansteen, A. Kimel, A. Kirilyuk, and T. Rasing, Femtosecond Photomagnetic Switching of Spins in Ferrimagnetic Garnet Films, *Phys. Rev. Lett.* **95**, 047402 (2005).
- [9] G. P. Zhang, T. Latta, Z. Babyak, Y. H. Bai, and T. F. George, All-optical spin switching: A new frontier in femtomagnetism – A short review and a simple theory, *Mod. Phys. Lett. B* **30**, 16300052 (2016).
- [10] G. P. Zhang, M. Gu, and X. S. Wu, Ultrafast reduction in exchange interaction by a laser pulse: alternative path to femtomagnetism, *J. Phys.: Condens. Matter* **26**, 376001 (2014).
- [11] H. Brune, Assembly and Probing of Spin Chains of Finite Size, *Science* **312**, 1005 (2006).
- [12] M. A. Norcia, R. J. Lewis-Swan, J. R. K. Cline, B. Zhu, A. M. Rey, and J. K. Thompson, Cavity-mediated collective spin-exchange interactions in a strontium superradiant laser, *Science* **361**, 259 (2018).
- [13] E. Jaynes and F. Cummings, Comparison of quantum and semiclassical radiation theories with application to the beam maser, *Proc. IEEE* **51**, 89 (1963).
- [14] M. Tavis and F. W. Cummings, Exact Solution for an N -Molecule-Radiation-Field Hamiltonian, *Phys. Rev.* **170**, 379 (1968).
- [15] R. H. Dicke, Coherence in Spontaneous Radiation Processes, *Phys. Rev.* **93**, 99 (1954).
- [16] P. Kirton, M. M. Roses, J. Keeling, and E. G. Dalla Torre, Introduction to the Dicke Model: From Equilibrium to Nonequilibrium, and *Vice Versa*, *Adv. Quantum Technol.* **2**, 1800043 (2019).
- [17] K. D. B. Higgins, S. C. Benjamin, T. M. Stace, G. J. Milburn, B. W. Lovett, and E. M. Gauger, Superabsorption of light via quantum engineering, *Nature Communications* **5**, 4705 (2014).
- [18] H. Grinberg, Beyond the rotating wave approximation. An in-

- tensity dependent nonlinear coupling model in two-level systems, *Phys. Lett. A* **374**, 1481 (2010).
- [19] S. Agarwal, S. M. H. Rafsanjani, and J. H. Eberly, Tavis-Cummings model beyond the rotating wave approximation: Quasidegenerate qubits, *Phys. Rev. A* **85**, 043815 (2012).
- [20] G. Agarwal, R. Puri, and R. Singh, Atomic Schrödinger cat states, *Phys. Rev. A* **56**, 2249 (1997).
- [21] A. Klimov and C. Saavedra, The Dicke model dynamics in a high detuning limit, *Phys. Lett. A* **247**, 14 (1998).
- [22] C. Sträter, O. Tsypliyatyev, and A. Faribault, Nonequilibrium dynamics in the strongly excited inhomogeneous Dicke model, *Phys. Rev. B* **86**, 195101 (2012).
- [23] T. Tokihiro, Y. Manabe, and E. Hanamura, Superradiance of Frenkel excitons in linear systems, *Phys. Rev. B* **47**, 2019 (1993).
- [24] N. Wu, J. Feist, and F. J. Garcia-Vidal, When polarons meet polaritons: Exciton-vibration interactions in organic molecules strongly coupled to confined light fields, *Phys. Rev. B* **94**, 195409 (2016).
- [25] N. Wu, Determinant representations of spin-operator matrix elements in the XX spin chain and their applications, *Phys. Rev. B* **97**, 014301 (2018).
- [26] H. Tonchev, A. A. Donkov, and H. Chamati, Interaction of a single mode field cavity with the 1D XY model: Energy spectrum, *J. Phys. Conf. Ser.* **682**, 012032 (2016); Energy spectra of a spin- $\frac{1}{2}$ XY spin molecule interacting with a single mode field cavity: Numerical study, *J. Phys. Conf. Ser.* **764**, 012017 (2016); Energy spectra of a spin- $\frac{1}{2}$ XY spin molecule interacting with a single mode field cavity, *J. Phys. Conf. Ser.* **1186**, 012021 (2019).
- [27] E. Lieb, T. Schultz, and D. Mattis, Two soluble models of an antiferromagnetic chain, *Ann. Phys.* **16**, 407 (1961).
- [28] E. H. Lieb and D. C. Mattis, *Mathematical physics in one dimension: Exactly soluble models of interacting particles*. (Academic Press, New York, 1966).
- [29] A. De Pasquale, G. Costantini, P. Facchi, G. Florio, S. Pascazio, and K. Yuasa, XX model on the circle, *Eur. Phys. J. Spec. Top.* **160**, 127 (2008).
- [30] Below we use the notations of Wu [25].
- [31] We silently set $\sigma = -1$ between the projectors.
- [32] The formula for the transition matrix elements is first given in [23]. Another derivation is published later in [25].
- [33] For superradiance of a similar model system see also ([23]).
- [34] K. D. B. Higgins, S. C. Benjamin, T. M. Stace, G. J. Milburn, B. W. Lovett, and E. M. Gauger, Superabsorption of light via quantum engineering, *Nat. Commun.* **5**, 4705 (2014).
- [35] R. R. Puri, *Mathematical Methods of Quantum Optics*, edited by W. T. Rhodes, Springer Series in Optical Sciences, Vol. 79 (Springer Berlin Heidelberg, Berlin, Heidelberg, 2001).
- [36] Hereafter we will refer to this term as to a field-boundary XY term in the sense that it describes the coupling between the interacting and noninteracting with the field mode parts of the XY chain. It must not be confused with the boundary terms defined by the ends of the chain.
- [37] This is nonnegligible in the case near resonance.
- [38] This is nonnegligible in the case of large ω .
- [39] This is true when $(\alpha_+ \Omega T)^{-1}$ is not very large.
- [40] Here we skip the number operator for the sake of brevity.